NOISE REMOVAL IN ECG

DISSERTATION

SUBMITTED IN PARTIAL FULFILLMENT OF THE
REQUIREMENTS
FOR THE AWARD OF THE DEGREE
OF

MASTER OF TECHNOLOGY
IN
SIGNAL PROCESSING AND DIGITAL DESIGN

Submitted by:

AKHILESH KUMAR

(ROLL No. 2K11/SPD/19)

Under the supervision of

Mr.M.S.CHOUDHARY

DEPARTMENT OF ELECTRONICS AND COMMUNICATION ENGINEERING
DELHI TECHNOLOGICAL UNIVERSITY
(Formerly Delhi College of Engineering)
Bawana Road, Delhi-110042

2014

DECLARATION BY THE CANDIDATE

I hereby declare that the work presented in this dissertation titled " **Noise Removal in ECG**" has been carried out by me under the guidance of Mr. M.S.Chaudhary ,Associate Professor, Department of Electronics & Communication Engineering, Delhi technological University, Delhi and hereby submitted for the partial fulfillment for the award of degree of Master of Technology in Signal processing and Digital Design at Electronics & Communication Engineering Department , Delhi technological University, Delhi. I further undertake that the work embodied in this major project has not been submitted for the award of any other degree.

AKHILESH KUMAR
M.Tech.(Signal Processing & Digital Design)
Roll No. 2K11 / SPD / 19
Department of Electronics & Communication Engineering,
Delhi technological University,New Delhi-110042

DEPARTMENT OF ELECTRONICS AND COMMUNICATION ENGINEERING

DELHI TECHNOLOGICAL UNIVERSITY

(Formerly Delhi College of Engineering)

Bawana Road, Delhi-110042

CERTIFICATE

I, Akhilesh Kumar, Roll No. 2K11/SPD/19 student of M. Tech. (Signal Processing and Digital Design), hereby declare that the project titled "Noise Removal in ECG" under the supervision of Mr. M.S.Choudhary of Electronics and Communication Engineering Department, Delhi Technological University in partial fulfillment of the requirement for the award of the degree of Master of Technology has not been submitted elsewhere for the award of any Degree.

Place: Delhi **AKHILESH KUMAR**

Date: 27.07.2014

(M.S.CHOUDHARY)

Associate Professor

ABSTRACT

This project has been inspired by the need to find an efficient method for ECG Signal denoising using different combinations of wavelets and thresholding techniques. In this thesis , the ECG signal was decomposed in three level and reconstructed using different wavelet like Haar,Daubenchies,Symlet,Coiflets, BiorSpline, Reversebior, Demyer etc. and thresholding techniques. After that Notch Filter was applied for removing 50 Hz Power Line Noises. All the de-Noised ECG was calculated in terms of SNR, MSE and Cross correlations and summarized and compared the results.

ACKNOWLEDGEMENT

I would like to express my distinct pleasure and deep sense of gratitude and indebtedness to My project guide **Associate Professor M.S. Choudhary** for his counsel and guidance. I am thankful to him for the time and valuable advice he has given to me.

I am thankful to my parents and my wife Mamta for their motivation and support.

Last but not the least ,I offer my thanks to all my friends specially Mr. Raj Kumar Yadav and Mr.Akshya Sharma who have offered me help whenever I needed and have been a source of comfort.

Above all ,I am grateful to **GOD** for being with me and showing me the right path.

AKHILESH KUMAR

M.Tech.(Signal Processing & Digital Design)
Roll No. 2K11 / SPD / 19
Department of Electronics & Communication Engineering,
Delhi technological University,New Delhi-110042

CONTENTS

1. Introduction

Electrocardiogram (ECG) is a nearly periodic signal that reflects the activity of the heart. A lot of information on the normal and pathological physiology of heart can be obtained from ECG. However, the ECG signals being non-stationary in nature, it is very difficult to visually analyze them. Thus the need is there for computer based methods for ECG signal Analysis.

A lot of work has been done in the field of ECG signal Analysis using various approaches and methods. The basic principle of all the methods however involves transformation of ECG signal using different transformation techniques including Fourier Transform, Hilbert Transform, Wavelet transform etc. Physiological signals like ECG are considered to bequasi-periodic in nature. They are of finite duration and non stationary. Hence, a technique like Fourier series (based on sinusoids of infinite duration) is inefficient for ECG. On the other hand, wavelet, which is a very recent addition in this field of research, provides a powerful tool for extracting information from such signals. There has been use of both Continuous Wavelet Transform (CWT) as well as Discrete Wavelet Transform (DWT). However CWT has some inherent advantages over DWT. Unlike DWT, there is no dyadic frequency jump in CWT. Moreover, high resolution in time-frequency domain is achieved in CWT .

Transmission of ECG often results in the corruption of signal due to introduction of noise. Various factors responsible for introduction of noise include poor channel conditions, Baseline wander (caused by respiration), 50 or 60 Hz power line interference etc. Analyzing such a noisy signal is bound to give erroneous results. Thus the signal is first made free of noise, a process called denoising or rather we may call it enhancement. A number of methods have been incorporated for enhancement ECG signal. These include use of filter banks, neural network, adaptive filtering,notch filter etc.

Theoretical Concept of ECG

Heart

The heart, located in the mediastinum, is the central structure of the cardiovascular system. It is protected by the bony structures of the sternum anteriorly, the spinal column posteriorly, and the rib cage.

Sinoatrial (SA)

Sinoatrial node is the dominant pacemaker of the heart, located in upper portion of right atrium. It has an intrinsic rate of 60–100 bpm.

Atrioventricular(AV)

Atrioventricular node is a part of AV junctional tissue. It slows conduction, creating a slight delay before impulses reach ventricles. It has an intrinsic rate of 40–60 bpm.

Electrophysiology

Action	Effect
Depolarization	Shifting of electrolytes across the cell membrane causes change in electric charge of the cell. It results in contraction.
Repolarization	Internal negative charge is restored and the cells return to their resting state.

Conduction System Structure and Functions

Structure	Function and Location
Sinoatrial (SA) Node	Dominant pacemaker of the heart, located in upper portion of right atrium. Intrinsic rate 60–100 bpm.
Internodal Pathways	Direct electrical impulses between SA and AV nodes.
Atrioventricular (AV) node	Part of AV junctional tissue. Slows conduction, creating a slight delay before impulses reach ventricles. Intrinsic rate 40–60 bpm.
Bundle of His	Transmits impulses to bundle branches. Located below AV node.
Left bundle Branch	Conducts impulses that lead to left ventricle.
Right bundle Branch	Conducts impulses that lead to right ventricle.
Purkinje system	Network of fibers that spreads impulses rapidly throughout ventricular walls. Located at terminals of bundle branches.

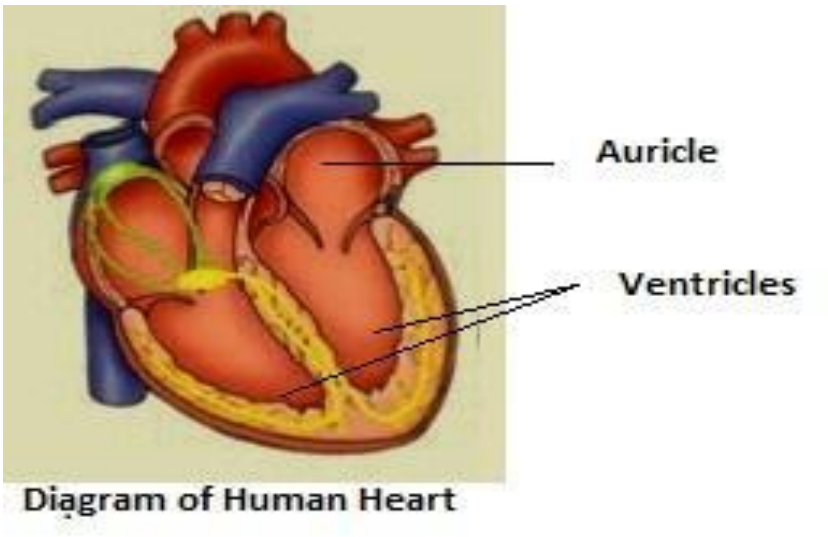

Fig.1

The Heart: Phases

There are two phases of the cardiac cycle .

Systole: The ventricles are full of blood and begin to contract. The mitral tricuspid valves close (between atria and ventricles). Blood is ejected through the pulmonic and aortic valves.

Diastole: Blood flows into the atria and through the open mitral and tricuspid valves into the ventricles.

Electrocardiogram (ECG)

An ECG is a series of waves and deflections recording the heart's electrical activity from a certain "view". Many views, each called a lead, monitor voltage changes between electrodes placed in different positions on the body.

Each cardiac cell is surrounded by and filled with solutions of Sodium (Na+), Potassium (K+), and Calcium (Ca++). The interior of the cell membrane is considered to be negative with respect to outside during resting conditions. When an electric impulse is generated in the heart, the interior part becomes positive with respect to the exterior. This change of polarity is called depolarization. After depolarization the cell comes back to its original state. This phenomenon is called repolarization. The ECG records the electrical signal of the heart as the muscle cells depolarize (contract) and repolarize.

A normal ECG signal is shown.

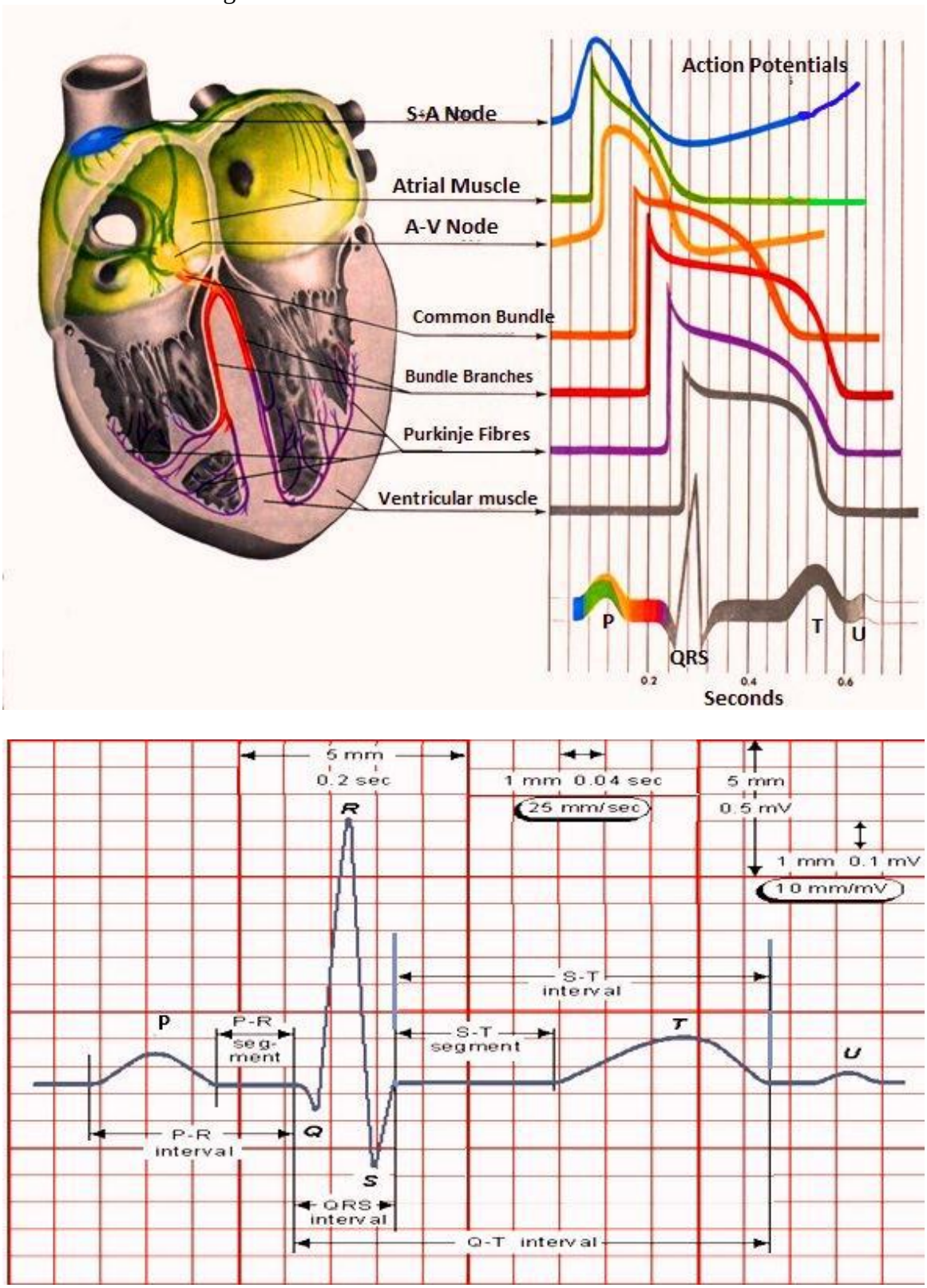

Fig,2. Normal ECG Signal and its various components

The impulses of the heart are recorded as waves called P-QRS-T deflections.
The following is the description and significance of each deflection and segment.

P wave indicates atrial depolarization (and contraction).
PR Interval measures time during which a depolarization wave travels from the atria to the ventricles.
QRS Interval includes three deflections following P wave which indicates ventricular depolarization (and contraction). Q wave is the first negative deflection while R wave is the first positive deflection. S wave indicates the first negative deflection after R wave.
ST Segment measures the time between ventricular depolarization and beginning of repolarization.
T wave represents ventricular repolarization.
QT Interval represents total ventricular activity.

Arrhytmia
Normally, the SA Node generates the initial electrical impulse and begins the cascade of events that result in a heart-beat. For a normal healthy person the ECG comes off as a nearly periodic signal with depolarization followed by repolarization at equal intervals. However, sometimes this rhythm becomes irregular.
Cardiac arrhythmia (also **dysrhythmia**) is a term for any of a large and heterogeneous group of conditions in which there is abnormal electrical activity in the heart. The heart beat may be too fast or too slow, and may be regular or irregular.
Arrthymia comes in varieties. It may be described as a flutter in chest or sometimes "racing heart". The diagnosis of Arrthymia requires Electrocardiogram. By studying ECG, Doctors can diagnose the disease and prescribe the required medications.

Measuring heat rate by using E.C.G:

Heart rate can be measured by e.c.g. outputs easily by counting the no. of big blocks b/w two successive R-waves as:-

Remember the sequence 300,150,100,75,60,50. If there is one big block it means heart rate is 300, for 2 big blocks its 150 and so on.

There are two phenomenon attached with the measurement of heart rate as given below:

Sinus bradycardia: if heart rate goes below 60.

Sinus tachycardia: if heart rate exceeds 100.

Normal Results

Heart rate: 50 to 100 beats per minute.

Rhythm: consistent and even.

Cardiac muscle has automaticity, which means that it is self-exciting. This is in contrast with skeletal muscle, which requires either conscious or reflex nervous stimuli for excitation. The heart's rhythmic contractions occur spontaneously, although the rate of contraction can be changed by nervous or hormonal influences, exercise and emotions. For example, the sympathetic nerves to heart accelerate heart rate and

the vagus nerve decelerates heart rate.

The rhythmic sequence of contractions is coordinated by the sinoatrial (SA) and atrioventricular (AV) nodes. The sinoatrial node, often known as the *cardiac pacemaker*, is located in the upper wall of the right atrium and is responsible for the wave of electrical stimulation that initiates atrial contraction by creating an action potential. Once the wave reaches the AV node, situated in the lower right atrium, it is delayed there before being conducted through the bundles of *His* and back up the Purkinje fibers, leading to a contraction of the ventricles.

The delay at the AV node allows enough time for all of the blood in the atria to fill their respective ventricles. In the event of severe pathology, the AV node can also act as a pacemaker; this is usually not the case because their rate of spontaneous firing is considerably lower than that of the pacemaker cells in the SA node and hence is overridden.

Why the Test is performed

An ECG is very useful in determining whether a person has heart disease. If a person has chest pain or palpitations, an ECG is helpful in determining if the heart is beating normally. If a person is on medications that may affect the heart or if the patient is on a pacemaker, an ECG can readily determine the immediate effects of changes in activity or medication levels. An ECG may be included as part of a routine examination in patients over 40 years old.

What Abnormal Results Mean

Abnormal ECG results may indicate the following:

- Myocardial (cardiac muscle) defect
- Enlargement of the heart
- Congenital defects
- Heart valve disease
- Arrhythmias (abnormal rhythms)
- Tachycardia (heart rate too fast) or bradycardia (too slow)
- Ectopic heartbeat
- Coronary artery disease
- Inflammation of the heart (myocarditis)
- Changes in the amount of electrolytes (chemicals in the blood)
- Past heart attack
- Present or impending heart attack

Risks

There are generally no risks. Because this procedure merely monitors the electrical

impulses and does not emit electricity, there is no risk of shock.During an exercise electrocardiogram, some patients experience arrhythmias or heart distress. Equipment for dealing with these occurrences is located in the testing area.

Common symptoms that frequently require an ECG include the following:

- Chest pain or discomfort
- Shortness of breath
- Nausea
- Weakness
- Palpitations (rapid or pounding heartbeats or increased awareness of heart beating)
- Anxiety
- Abdominal pain
- Fainting (syncope)

Considerations

The accuracy of the ECG varies with the condition being tested. Some heart conditions are not detectable all the time, and others may never produce any specific ECG changes.

A person who suspects heart disease or has had a heart attack may need more than one ECG. There is no reason for healthy people to undergo annual testing unless they have inherited risks or a medical condition.

It is important to be relaxed and relatively warm during ECG recording. Any movement, including muscle tremors such as shivering, can alter the tracing.

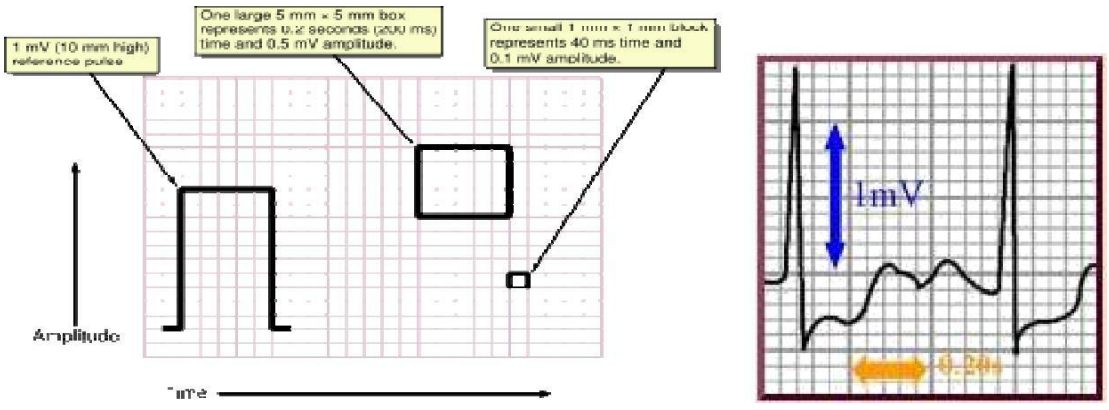

Fig. 3 E.C.G Graph Paper

A typical electrocardiograph runs at a paper speed of 25 mm/s, although faster paper speeds are occasionally used. Each small block of ECG paper is 1 mm². At a paper speed of 25 mm/s, one small block of ECG paper translates into 0.04 s (or 40 ms). Five small blocks make up 1 large block, which translates into 0.20 s (or 200 ms). Hence, there are 5 large blocks per second. A diagnostic quality 12 lead ECG is calibrated at 10 mm/mV, so 1 mm translates into 0.1 mV.

The Duration of the Complexes and Intervals

After determining the heart rate and rhythm, the clinician should measure the duration of the waves and intervals on the electrocardiogram.

The P wave: The duration of the P wave is measured from the beginning of the P wave to the end. In normal adults, this period is usually less than 0.12 second; in neonates, it is less than 0.08 second. This is the time interval required for the wave of depolarization to spread through the atria and to reach the atrioventricular node. The amplitude of the P waves of the normal adult is less than 0.25 mV in the extremity leads and smaller than this in children.

The PR interval: The PR interval represents the amount of time required for the depolarization process to spread from its origin in the sinus node, through the atria, to and through the atrioventricular node (where the impulses are delayed), down the bundle
branches and their sub-branches (including the Purkinje fibers), and to the ventricular muscle. It is measured from the beginning of the P wave to the beginning of the QRS complex. In reality, this interval should be called the PQ interval, but convention holds that it is called the PR interval.

When there is no Q wave, the measurement is made from the beginning of the P wave to the beginning of the R wave. The difference between the intervals as measured to the beginning of the Q wave, and as measured to the R wave, is usually about 0.02 second but may be as much as 0.04 second. The PR interval is less than 0.20 second in the normal adult and much less than this in normal children.

The duration of the QRS complex: The duration of the QRS complex represents the amount of time required for the depolarization of the ventricular musculature. It is measured from the beginning of the Q wave to the end of the S wave. In normal adults, the QRS duration is usually 0.10 second or less and in children, it is usually less than 0.08 second. When the QRS duration is greater than 0.10 second in adults, it is proper to consider the presence of some type of ventricular conduction defect.

QRS amplitude: The normal QRS voltage may be as small as 0.5 - 0.7 mV, but it is usually greater than this. It is generally accepted that the QRS voltage is definitely small, when it measures 0.4 mV or less in all the extremity leads. When this occurs, it is wise to consider certain abnormalities as possible causes.

The duration of the ST segment: The duration of the ST segment represents the amount of time during which the ventricular musculature is depolarized. The depolarization process ends with the end of the QRS complex, and the repolarization

begins with, or before, the beginning of the T wave. In some patients, the repolarization process begins during the ST segment.

The ST segment duration is determined by measuring the interval of time from the end of the S wave to the beginning of the T wave. In practice, a prolonged ST segment is identified by detecting a prolonged QT interval, while the duration of the T wave remains normal.

The QT interval: The QT interval represents the amount of time required for depolarization of the ventricles, plus the amount of time during which the ventricles are excited (ST segment), plus the amount of time required for their repolarization (T wave).

This interval represents the duration of electrical systole, which is different from the duration of mechanical systole. The QT interval is measured from the beginning of the Q wave of the QRS complex to the end of the T wave. The duration of the QT interval varies with age, gender, and heart rate. It should not exceed 0.40 second, when the heart rate of an adult is 70 depolarizations per minute.

The duration of the T wave: The T wave is produced by the repolarization process. The duration of the T wave is measured from the beginning of the wave to the end. The repolarization process undoubtedly begins before the T wave and is sometimes quite visible as a displaced ST segment, which is referred to as "early repolarization." Although the duration of the normal T wave has been studied, and tables have been constructed using the data, the actual measurement is rarely performed in practice.

The magnitude of the T wave: The area encompassed by the T wave may be a little smaller or a little larger than that encompassed by the QRS complex; it is usually about two-thirds that of the latter. Characteristically, the upstroke of the normal T wave is less steep than the downstroke.

The TQ interval. The TQ interval is measured from the end of the T wave to the beginning of the next Q wave. During this period the ventricles are polarized and waiting for the stimulation that initiates depolarization.

• The Heart Rate and Rhythm

Determination of the heart rate and rhythm. Normally, the heart of an adult is depolarized 60 to 90 times per minute. A depolarization rate lower than this is called sinus bradycardia, while one that is higher is called sinus tachycardia. The heart rate of the normal newborn is much higher than that of an adult. The heart rate can be calculated by dividing the R-R interval into 60. This number is denoted BPM (Beats per Minute).

- **<u>Arrhythmias</u> (Abnormal Patterns)**

The clinician who uses the electrocardiogram as a diagnostic test wishes to determine cardiac abnormalities from the body surface potentials. As a rough framework, it is worth thinking of the heart as three separate systems: a functional electrical system, a functional system of *coronary* (or cardiac) arteries to channel nourishing blood to every cell of the myocardium, and a culmination in an effective mechanical pump.

First we consider how an ECG is used to assess electrical abnormalities of the heart. The surface ECG has inherent limitations as a diagnostic tool: Given a distribution of body surface potentials, we cannot precisely specify the detailed electrophysiologic behavior of the source since this *inverse* problem does not have a unique solution (as demonstrated in 1853 by Hermann von Helmholz).

It is not, in general, possible to uniquely specify the characteristics of a current generator from the external potential measurements alone. Therefore, an exacting assessment of the electrical activity of the heart involves an invasive electrode study. Despite these inherent
limitations, the surface ECG is extremely useful in clinical assessments of electrical pathologies and an invasive electrophysiologic study is indicated in only a small fraction of cases.

To a first approximation, electrical problems come in two forms: those which make the heart pump too slowly or infrequently (bradycardias), and those with make the heart pump too quickly (tachycardias). If the pumping is too slow, the cardiac output of life-sustaining blood can be dangerously low. If too quick, the cardiac output can also be too low since the heart does not have time to fill, and also because the heart can suffer damage (e.g., *demand ischemia*) when it tries to pump too rapidly.

2. NOISE IN ELECTROCARDIOGRAMS

Electrocardiogram traces used for identification are obtained using surface electromyography (EMG), where electrodes are placed on the skin in the vicinity of the heart. Potential differences of 1 to 3 mV generated at the body surface by the current sources in the heart are picked up by the electrodes and are amplified in order to improve the signal to noise ratio (SNR). The ECG waveform is observed on an oscilloscope or is digitized for further processing by a computer (as will be the case for recognition purposes). The digitization process should use a sampling rate of at least 1 kHz to ensure that the ECG trace is of a high enough resolution as required for biometric purposes [1].

ECG measurements may be corrupted by many sorts of noise. The ones of primary interest are:

1. power line interference,

2. electrode contact noise,
3. motion artifacts,
4. EMG noise, and
5. instrumentation noise [3].

An idealized block diagram of each of these noise sources is shown in Fig. 2. The various noise signals presented in the figure will be characterized in greater detail in this section.

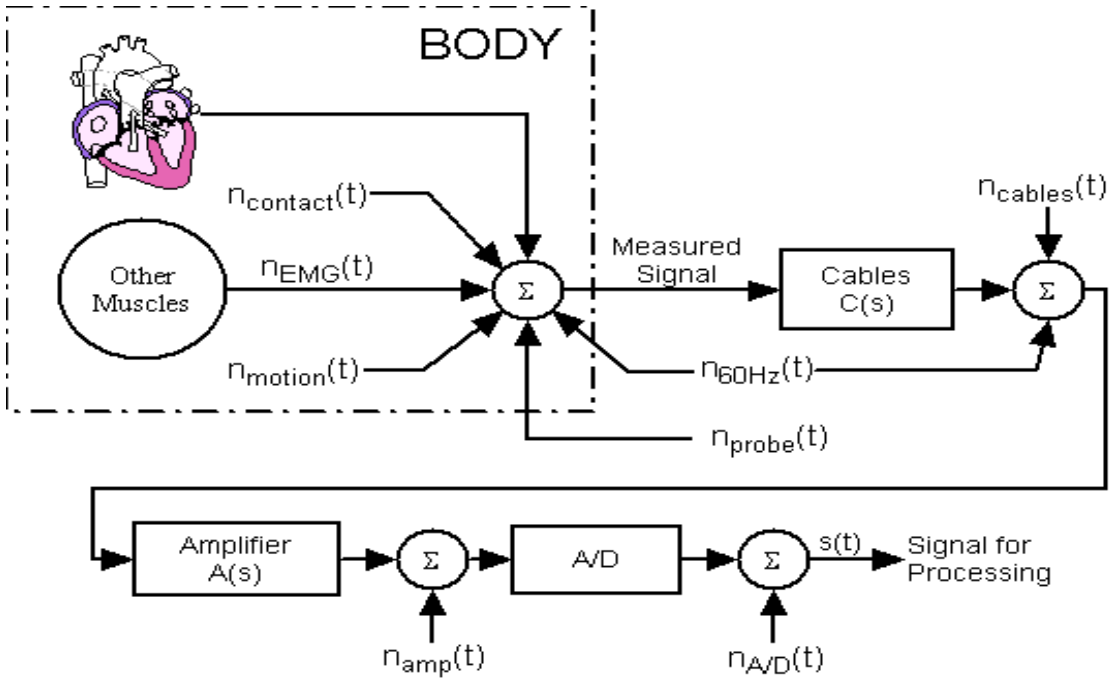

Fig. 4

A. Power Line Interference

Plotting a Fourier power spectrum of a typical ECG signal (Fig. 6) reveals various common ECG frequency components. Several interesting features are readily identifiable:

- The 1.2 Hz heart beat information (approximately 72 beats per minute)
- The 60 Hz power line interference

The remainder of the frequency components represents the subject information (situated between 0.1 Hz and 40 Hz) and contributions of other noise sources.

Power line interference occurs through two mechanisms: capcaitive and inductive coupling. Capacitive coupling referes to the transfer of energy between two circutis by means of a coupling capacitance present between the two ciricuits. The value of the coupling capacitance decreases with increasing separtion of the circuits. Inductive coupling on the other hand is caused by mutual inducatance between two conductors. When current flows through wires it produces a magnetic flux, which can induce a current in adjacent cirucits. The geometry of the conductors as well as the separtion between them determines the value of the mutual inductance, and hence the degree of the inductive coupling. Typically, capacitive coupling is responsible for high frequency noise while inductive coupling introduces low frequency noise. For this reason inductive coupling is the dominant mechanism of power line interference in

electrocardiology. Ensuring the electrodes are applied properly, that there are no loose wires, and that all components have adequate shielding should help limit the amount of power line intererence.

The manifestation of power line noise can be modeled by

$$n_{60Hz}(t) = A\sin(2\pi \cdot 60 + \Omega).$$

The average peak value, *A*, of the noise depends on the amount of coupling between the ECG equipment and the power lines, and will vary between measurements. During measurement the peak-to-peak value is also liable to fluctuate due to changing environmental conditions, which influence the amount of inductive or capacitive coupling of power lines to the ECG equipment. The phase of the sinusoid, represented by Ω in equation (1), is a random variable with a uniform distribution in the range [-π, π). This simplistic model assumes that the noise will occur only at 60 Hz, but in reality the power line noise will have a finite bandwidth around its nominal center frequency, suggesting that the total noise is composed of many sinusoids of similar frequency.

.

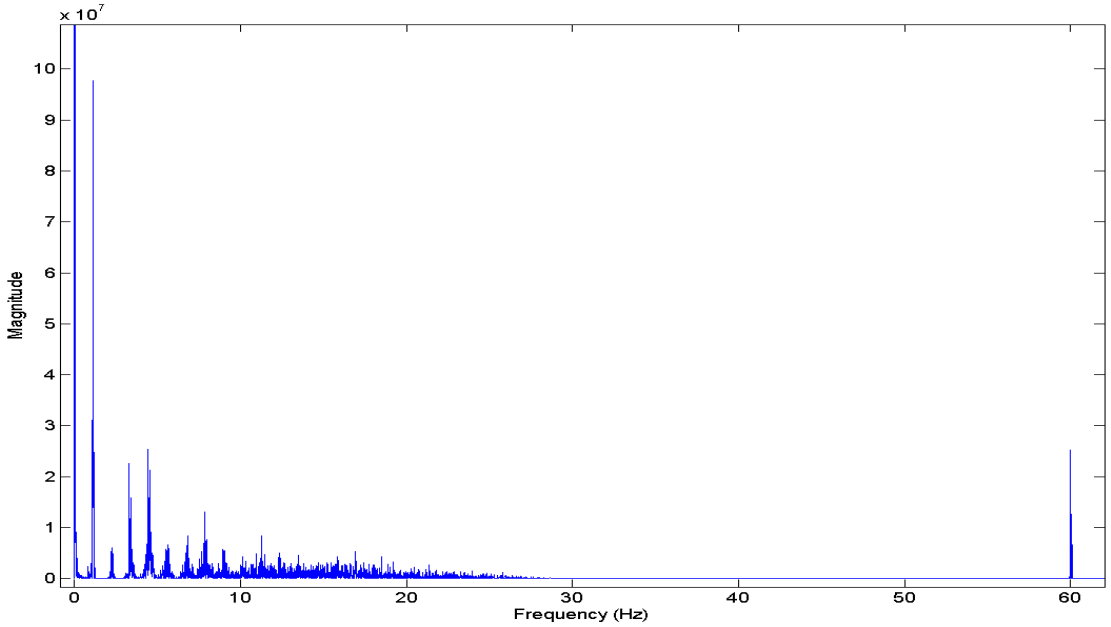

Fig 5 Fourier power spectrum of an ECG trace. The 60 Hz power line interference and the baseline potential drift noise (at approximately 0 Hz) are identifiable

B. Electrode Contact Noise and Motion Artifacts

Electrode contact noise is caused by variations in the position of the heart with respect to the electrodes and changes in the propagation medium between the heart and the electrodes. This causes sudden changes in the amplitude of the ECG signal, as well as low frequency baseline shifts. In addition, poor conductivity between the electrodes and the skin both reduces the amplitude of the ECG signal and increases the probability of disturbances (by reducing SNR). The underlying mechanism resulting in these baseline disturbances is electrode-skin impedance variation. The larger the

electrode-skin impedance, the smaller the relative impedance change needed to cause a major shift in the baseline of the ECG signal. If the skin impedance is

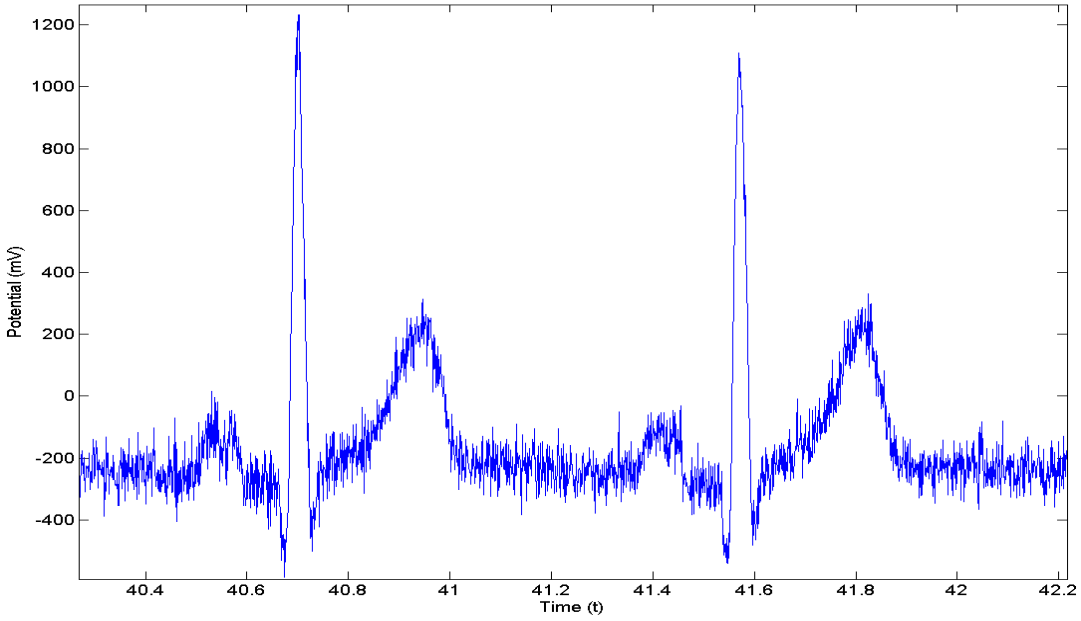

Fig. 6. Two second segment of an ECG trace. The *x*-axis is time in seconds, and the *y*-axis is the electrical potential in millivolts. Exact positions of P and T complexes are obscured be presence of EMG noise

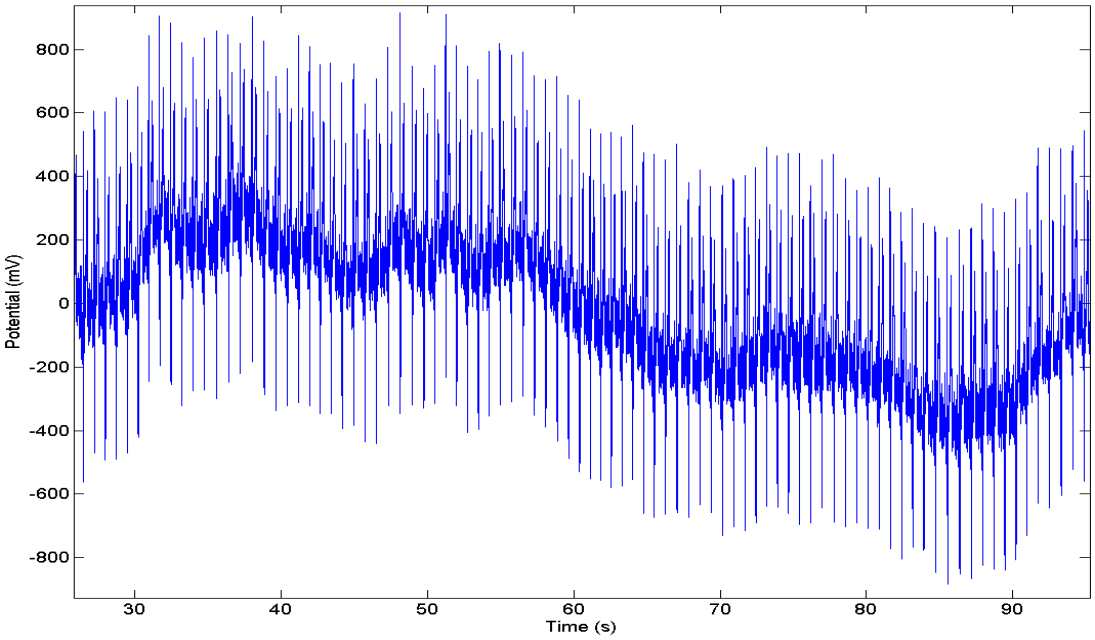

Fig. 7. Seventy seconds of ECG data. The *x*-axis is time in seconds, and *y*-axis is the electrical potential in millivolts. A baseline potential drift is present in the ECG trace

extraordinarily high, it may be impossible to detect the signal features reliably in the presence of body movement . Sudden changes in the skin-electrode impedance induce sharp baseline transients which decay exponentially to the baseline value. This

transition may occur only once or rapidly several times in succession. Characteristics of this noise signal include the amplitude of the initial transition and the time constant of the decay . The contact noise is represented by $n_{contact}(t)$ in Fig. 4.

Motion artifacts are transient (but not step) baseline changes caused by electrode motion. The usual causes of motion artifacts are vibrations, movement, or respiration of the subject. The peak amplitude and duration of the artifact are random variables which depend on the variety of unknowns such as the electrode properties, electrolyte properties (if one is used between the electrode and skin), skin impedance, and the movement of the patient . Fig. 4 shows a 70 second segment of a high resolution ECG trace, where the baseline drift varies from approximately -400mV to 400mV. In this ECG signal, the baseline drift occurs at an unusually low frequency (approximately 0.014Hz), and most likely results from very slow changes in the skin-electrode impedance. This noise can also be observed on the Fourier power spectrum in Fig. 6; the large peak nearest to DC is the result of very low frequency base line shifts. The noise artifacts introduced by subject motion are modeled by $n_{motion}(t)$

C. EMG Noise

EMG noise is caused by the contraction of other muscles besides the heart. When other muscles in the vicinity of the electrodes contract, they generate depolarization and repolarization waves that can also be picked up by the ECG. The extent of the crosstalk depends on the amount of muscular contraction (subject movement), and the quality of the probes.

It is well established that the amplitude of the EMG signal is stochastic (random) in nature and can be reasonably modeled by a Gaussian distribution function . The mean of the noise can be assumed to be zero; however, the variance is dependent on the environmental variables and will change depending on the conditions. Certain studies have shown that the standard deviation of the noise is typically 10% of the peak-to-peak ECG amplitude . While the actual statistical model is unknown, it should be noted that the electrical activity of muscles during periods of contraction can generate surface potentials comparable to those from the heart, and could completely drown out the desired signal. The effects of typical EMG noise can be observed in the ECG signal, and is particularly problematic in the areas of the P and T complexes. This noise is modeled by $n_{EMG}(t)$ in Fig. 1.

D. Instrumentation Noise

The electrical equipment used in ECG measurements also contributes noise. The major sources of this form of noise are the electrode probes, cables, signal processor/amplifier, and the Analog-to-Digital converter, represented respectively by $n_{probe}(t)$, $n_{cables}(t)$, $n_{amp}(t)$, and $n_{A/D}(t)$ in Fig. 4. Since this form of noise is usually defined by a white Gaussian distribution, Fig. 6 adequately represents its effects on the ECG signal. Unfortunately instrumentation noise cannot be eliminated as it is inherent in electronic components, but it can be reduced through higher quality equipment and careful circuit design.

One type of electrical noise is resistor thermal noise (also known as Johnson noise). This noise is produced by the random fluctuations of the electrons due to thermal agitation. The power spectrum of this noise is given by

$$\overline{V}_n^2 = 4kTR,$$

where k is the Boltzmann's constant, T is the temperature, and R is the resistance . This equation suggests that the resistor thermal noise is white for all frequencies; however, at frequencies larger than 100 THz the power spectrum starts to drop off. For our purposes we can assume the resistor thermal noise to be band limited white noise. This type of noise is generated in the electrodes, in the wire leads connecting electrodes to the amplifier, and in all the resistive electronic components internal to the ECG instrumentation. Since the magnitude of this noise component is substantial relative to the measured signal, its effects are most noticeable in the electrodes and any other electronic equipment prior to the amplifier.

Another form of noise, called flicker noise, is very important in ECG measurements, due to the low frequency content of ECG data. The actual mechanism that causes this type of noise is not yet understood, but one widely accepted theory is that it is caused by the energy traps which occur between the interfaces of two materials. It is believed that the charge carriers get randomly trapped/released and cause flicker noise. For MOSFET devices, the power spectral density of flicker noise is given by,

$$\overline{V}_{1/f}^2 = \frac{4kT}{WLC_{ox}f},$$

where k is the Boltzmann's constant, T is the temperature, C_{ox} is the silicon oxide capacitance, WL is the transistor area, and f is the frequency . As the equation suggests, flicker noise is inversely proportional to frequency, indicating that it becomes dominant at lower frequencies. It can be found in any electronic equipment which utilizes bipolar or metal oxide transistors, such as the amplifier used for signal amplification (or more specifically any device which has material junctions). Flicker noise contributions would be most noticeable at the electrodes since the amplitude of the detected signal is on the order of millivolts.

3. Literature Survey

Today signal processing plays a major role in ECG signal analysis and interpretation. The aim of ECG signal processing is diverse and comprises the Improvement of measurement accuracy and reproducibility (when compared with manual measurements) and by taking out the information is not readily available from the signal through visual assessment. A recorded ECG signal is a mixture of a signal and interference that may complicate computer signal delineation.

Before looking at different denoising techniques, it is essential to clarify what is meant by noise. Typically noise in a real-world data acquisition system has an unknown distribution. Some of the SNR and artifact problems that arise during these recordings can be suppressed by simple, frequency-selective filtering. But there are some disadvantages in that process . Transform without down sampling, is called stationary (redundant) wavelet transform (SWT), is more preferable for filtering. Thresholding using SWT Better results can be achieved by using the wavelet Wiener filtering, when each transform coefficient is adjusted separately. The Wiener filter requires an estimate of a noise-free signal, which is necessary to calculate the correction factor for the adjustment of transform coefficients. The principle of the

method was described in . The wavelet Wiener filtering (WWF) with decimation and with simplified estimation of the noise-free signal , SWT with estimation of the noise-free signal was used. The estimation was carried out with WT with decimation and hard Thresholding. Because the noise-free signal coefficients u_m (n) are unknown, we use estimated values u_m (n), which we get by pilot estimation method , another filter is derived using a Bayesian framework and constitutes a KALMAN filter in which the dynamic variations in the ECG are modeled by a covariance matrix that is adaptively estimated every time new data arrive . The filters were tested on signals with artificial noise, whose power spectrum was adapted to the spectrum of an ECG signal.

DIFFERENT DENOISING TECHNIQUES

The various methods of denoising that can be implemented for removal of noise available in the ECG signals are discussed below.

A. Wavelet Filtering Method (WF)

The simple Wavelet Filter is based on an appropriate adjustment of wavelet coefficients in the wavelet domain. With regard to the character of ECG wavelet coefficients, it is effective to separate the interference and the signal via Thresholding. Selecting proper Thresholding is important role in denoising ECG signal Effective Thresholding requires 1) to evaluate the right value of the threshold and 2) to choose the right methods of Thresholding.

1. *Threshold Level*: We suppose that the corrupted signal x (n) is an additive mixture of the noise-free signal $s(n)$ and the noise $w(n)$, $x(n) = s(n) + w(n)$, both uncorrelated, where n represents the discrete time ($n = 0, 1, \ldots, N-1$) and N is the length of the signal. If we transform the noisy signal $x(n)$, using the linear dyadic SWT, into the wavelet domain, we obtain the wavelet coefficients y_m $(n) = u_m$ $(n) + v_m$ (n), where u_m (n) are the coefficients of the noise-free signal and v_m (n) are the coefficients of the noise, and m is the level of decomposition which denotes the m^{th} frequency band. The threshold levels for the modification of the wavelet co-efficient should be set separately for each decomposition level m with respect to the noise level v_m (n) (its standard deviation σ_{vm}). In the case of lower noise level, the threshold level is lower and the corruption of the noise-free signal is also lower. The issue of the wavelet Thresholding is described in .There is many methods for estimating the optimal Threshold values.

2. *Right method of Thresholding- (a) Universal Thresholding:* This is proposed by Donoho. The threshold

value is given by $\sqrt{2\log(n)}$

Where, n is the number of samples in the signal.

- *Hard Thresholding:* This is proposed by Donoho. Due to the discontinuities of the shrinkage function, hard shrinkage estimates tend to have a bigger variance. In other words, it will be sensitive to small changes in the signal. And it is given by equation

$$Y = \begin{cases} 0, & [y] < Thr \\ y, & [y] \geq Thr \end{cases}$$

• *Soft Thresholding:* This method is proposed by Johnston. The derivation of standard soft shrinkage function is not continuous. The soft shrinkage estimates tend to have a bigger bias, due to the shrinkage of large coefficients. It is given by equation

$$\begin{cases} 0 & [y] < Thr \\ y - Thr & [y] > Thr \\ y + Thr & [y] < Thr \end{cases}$$

B. Wavelet Wiener Filtering Method (WWF)

From the coefficients y_m (n), we are able to estimate the noise-free coefficients u_m (n), using the WWF method, which is based on the Wiener filtering theory applied in the wavelet domain. The procedure is illustrated in Fig.. The upper path of the scheme consists of four blocks: the wavelet transforms SWT1, the modification of the coefficients in block H; the inverse wavelet transforms ISWT1, and the wavelet transform SWT2. The first three blocks mentioned represent the classic Wavelet Filtering method described previously. The lower path of the scheme consists of three blocks: the wavelet transform SWT2, the Wiener filter in the wavelet domain HW, and the inverse wavelet transform ISWT2. Using the inverse transform ISWT1, we get the estimate sˆ (n), which approximates the noise-free signal s(n). This estimate is

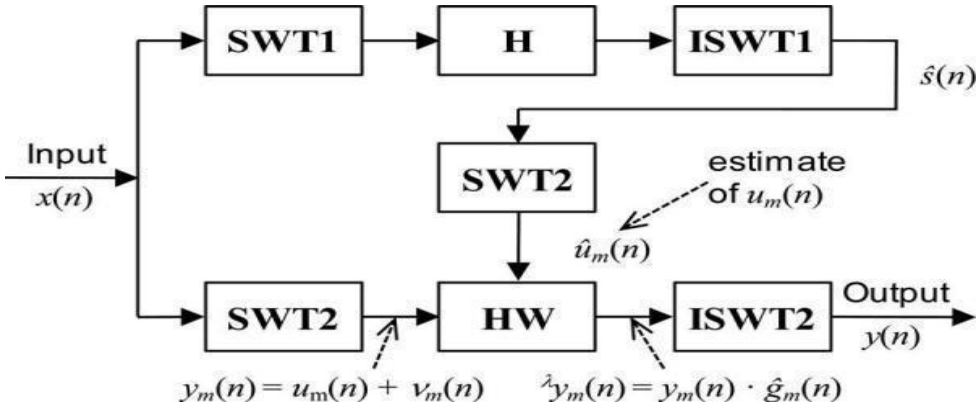

Fig.8. Block diagram of the WWF method, the upper path is used to estimate the noise-free signal ⁻(n) the lower path implements the Wiener filter in the wavelet domain

Used to design the Wiener Filter (HW), which is applied to the original noisy signal *x*(*n*) in the SWT2 domain (lower path), via the Wiener correction factor

$\hat{g}_m(n) = \hat{u}^2_m(n) / \hat{u}^2_m(n) + \sigma^2_{vm}(n)$

Where $\hat{u}^2_m(n)$ are the squared wavelet coefficients obtained from the estimate $\hat{s}(n)$, and $\sigma_v{}^2_m(n)$ is the variance of the noise coefficients $v_m(n)$ in the m^{th} band. We process the noisy coefficients $y_m(n)$ in the HW block, using the previously described Wiener correction factor, to obtain the modified coefficients

$$^{\lambda} y_m(n) = y_m(n) \cdot \hat{g}_m(n)$$

The output signal $y(n)$ is obtained by the ISWT2 inverse transform of the modified coefficients $^{\lambda} y_m(n)$.

C. Adaptive Wavelet Wiener Filtering Method (AWWF)

The WWF method has many parameters, which have to be set manually.

The most important ones are the decomposition level of the WT, the Thresholding method in the wavelet domain, the threshold multiplier, and the wavelet filter banks used in the SWT1 and SWT2 transforms. The appropriate setting of the input parameters has a great influence on the filtering results. Unfortunately, it is not clear which parameters should be used for ECG signal denoising. Moreover, it is obvious that for different noise levels present in the input signal different settings of the input parameters are suitable. Therefore, a robust filtering algorithm should be changing its parameters depending on the actual amount of noise. We improved the WWF method by adding the block for noise estimate (NE), as can be seen in Fig. 3. This block needs two inputs: the first is the noisy signal $x(n)$ and the second is the estimate of the noise-free signal $y(n)$ obtained by the WWF method with universal parameters (more in Section II-E3). The difference of these two signals gives an estimate of the input noise and we can calculate the SNR. The parameters in blocks SWT3, H3, ISWT3, SWT4 and ISWT4 are set up using the estimated SNR value. The remaining problem is that we do not know yet the correct setting of the individual blocks. Therefore, it was necessary to find these parameters individually for different levels of interference.

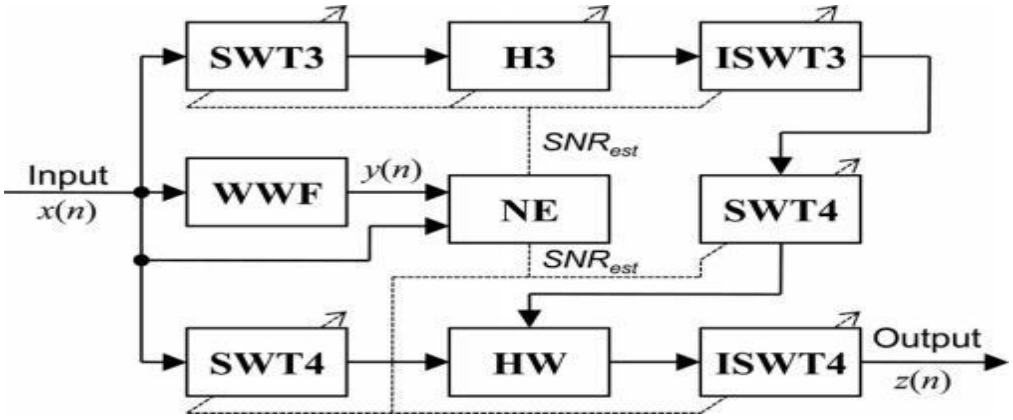

Fig.3. Block diagram of the AWWF method. The most important block is NE, where the SNR is estimated. According to this estimate all the relevant parameters are set.

In the upper part is an input ECG signals, the lower part is an estimate of noise. We can see that the signal is divided into three segments, each with an approximately constant level of interference. The example of signal comes from the CSE database.

D. Pilot Estimation Method

By careful input signal pre-processing using wavelet transform and Thresholding we obtain estimation of coefficients $u_m(n)$. Block diagram is in Figure 4. There is realized wavelet transform WT1 in the upper branch, modification of coefficients in the block H and inverse transform IWT1.Result is pilot signal s(n), which approximate noise-free signal s(n).

Input signal x(n) and also pilot signal s(n) enter to the transform WT2. Block HW process both outputs from WT2 by correction factor where 2 um n are square DTWT coefficients obtained from pilot estimation s(n).We get final signal y(n) by inverse transform IWT2 of modified coefficients $\lambda y_m(n)$.

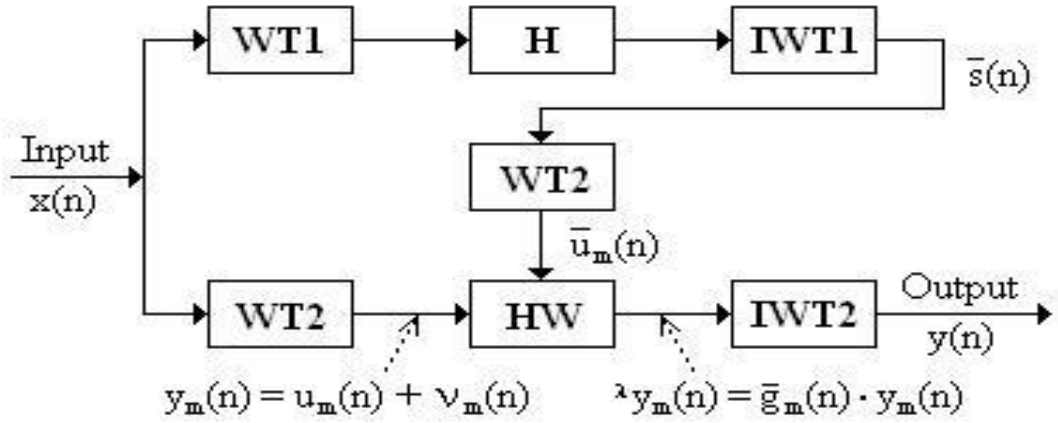

Figure 4: Block diagram of pilot estimation method.

Realization of pilot estimation is placed on upper branch: At first the input signal is decomposed by DTWT (WT1) into 4 levels. Than the coefficients is threshold (block H) and reconstructed by inverse DTWT (IWT1). Output of this configuration give the pilot estimation p s(n) of the signal. Wavelet-based Wiener filtering is illustrated on the lower branch. Input signal is decomposed into 4 levels by block WT2, coefficients are modified by equations (block HW), where the $u_m(n)$ are replaced by pilot estimation p $u_m(n)$ obtained from decomposition of pilot signal estimation ps(n) by block WT2. Output of the modification block HW is signal named p $y_m(n)$. Finally the inverse IWT2 is necessary to complete reconstruction of the signal s(n).

E. Adaptive KALMAN Filter-Bayesian Model

Typically, ECG complexes that originate from consecutive heartbeats are very similar but not identical. Moreover, when recording the ECG, the signals are corrupted to some extent by noise and artifacts. In a simplified form, both the relation between consecutive ECG complexes and the corruption of the recorded ECG can be described by means of a state-space model where x_k denotes the [$T \times 1$] ECG complex for heartbeat k and y_k denotes the [$T \times 1$] recorded signal where T is the length of the ECG complex. The isolation of individual ECG complexes from the recorded signals is discussed in Section III-C. Also in this section, the choice for T and the implicit assumption of equal lengths for all ECG complexes is discussed. The evolution of the

ECG complexes between heartbeats is modeled by the [$T \times 1$] stochastic component v_k (also referred to as the process noise).

4. Methodology

4.1 Time-Frequency Analysis Methods

Great progress has been made in applying linear time-invariant techniques in signal processing. In such cases the deterministic part of the signal is assumed to be composed of complex exponentials, the solutions to linear time invariant differential equations. However, many biomedical signals do not meet these assumptions. Thus, the emerging techniques of time-frequency analysis can provide new insights into the nature of biological signals.

There are several different time frequency analysis methods such as short time Fourier transform, S transform, Wigner transform, and Cohen's distribution. I would focus on Cohen's class distribution since it is used in biomedical signals analysis more commonly than S transform. As for short time Fourier transform, it is also a popular analysis tool.

4.2 Wavelet Transforms

To extract information from signals and reveal the underlying dynamics that corresponds to the signals, proper signal processing technique is needed. Typically, the process of signal processing transforms a time domain signal into another domain since the characteristic information embedded within the time domain is not readily observable in its original form. Mathematically, this can be achieved by representing the time domain signal as a series of coefficients, based on a comparison between the signal x(t) and template functions $\{\mathbf{\Psi_n^*}(t)\}$.

$$\mathbf{c_n} = \int_{-\infty}^{\infty} \mathbf{x(t)\Psi_n^*(t)dt}$$

The inner product between the two functions x(t) and $\mathbf{\Psi_n^*}$ (t) is

$$\mathbf{\langle x, \Psi_n \rangle} = \int \mathbf{x(t)\Psi_n^*(t)dt}$$

The inner product describes an operation of comparing the similarity between the signal and the template function, i.e. the degree of closeness between the two functions. This is realized by observing the similarities between the wavelet transform and other commonly used techniques, in terms of the choice of the template functions. A non stationary signal is shown in Figure 2 as an example. The signal consists of four groups of impulsive signal trains. In these groups, the signals are composed of two major frequencies, 650 and 1500 Hz.

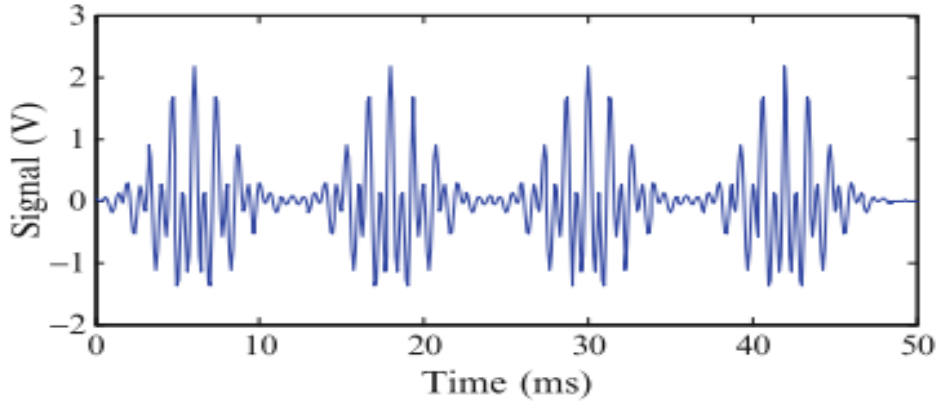

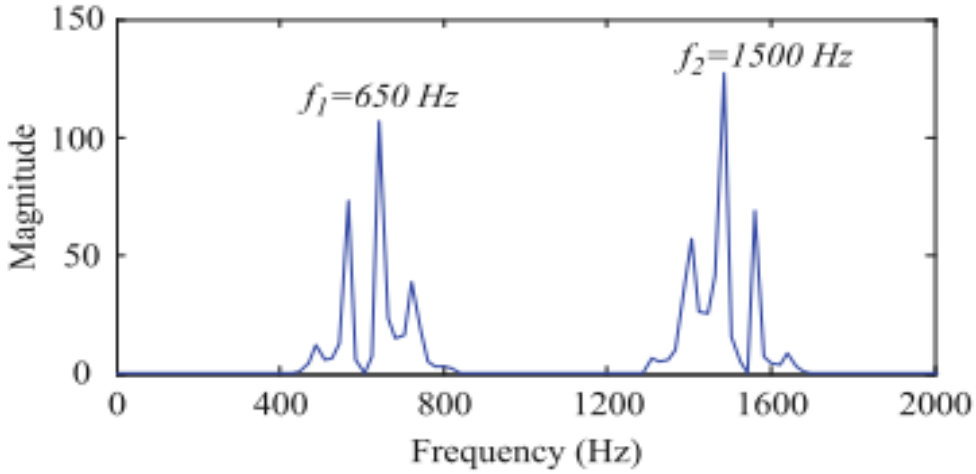

4.3 From Fourier to Wavelet Transform

Fourier Transform

Using the notation of inner product, the Fourier transform of a signal can be expressed as

$$\mathbf{X(f) = \langle x, e^{i2\pi ft} \rangle = \int_{-\infty}^{\infty} x(t) e^{-i2\pi ft}\, dt}$$

Assuming that the signal has finite energy

$$\mathbf{x(t) = \int_{-\infty}^{\infty} X(f) e^{i2\pi ft}\, df}$$

The Fourier transform is essentially a convolution between the time series x(t) and a series of sine and cosine functions that can be viewed as template functions. The operation measures the similarity between x(t) and the template functions, and

expresses the average frequency information during the entire period of the signal analyzed as shown in Figure

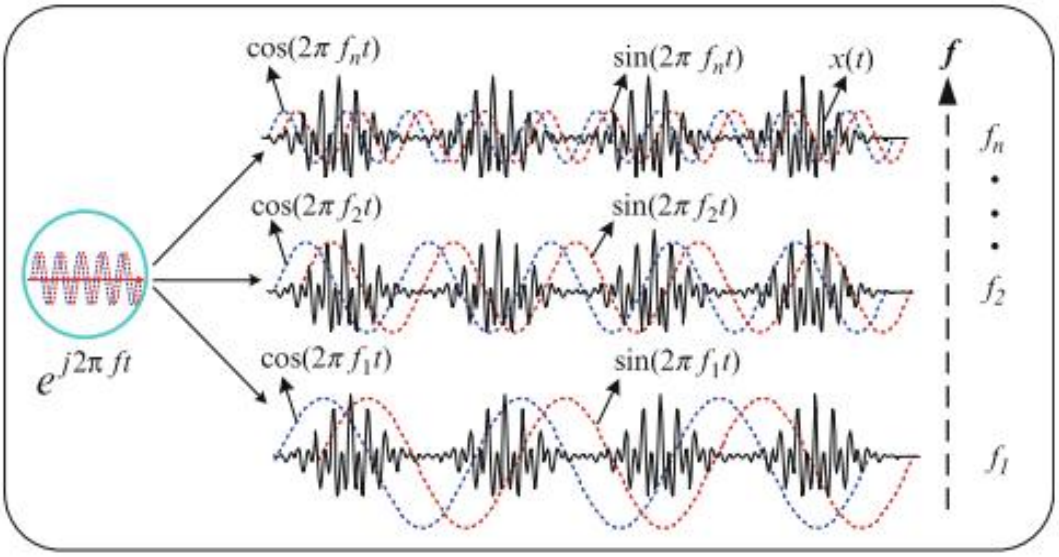

However, it does not reveal how the signal's frequency contents vary with time; that is, it does not reveal if two frequency components are present continuously throughout the time of observation or only at certain intervals, as is implicitly shown in the time-domain representation. Because the temporal structure of the signal is not revealed, the merit of the Fourier transform is limited; it is not suited for analyzing non stationary signals.

4.4 Short Time Fourier Transform

In Figure , the STFT employs a sliding window function g(t). A time-localized Fourier transform performed on the signal within the window. Subsequently, the window is removed along the time, and another transform is performed. The signal segment within the window function is assumed to be stationary. As a result, the STFT decomposes a time signal into a 2D time-frequency domain, and variations of the frequency within the window function are revealed.

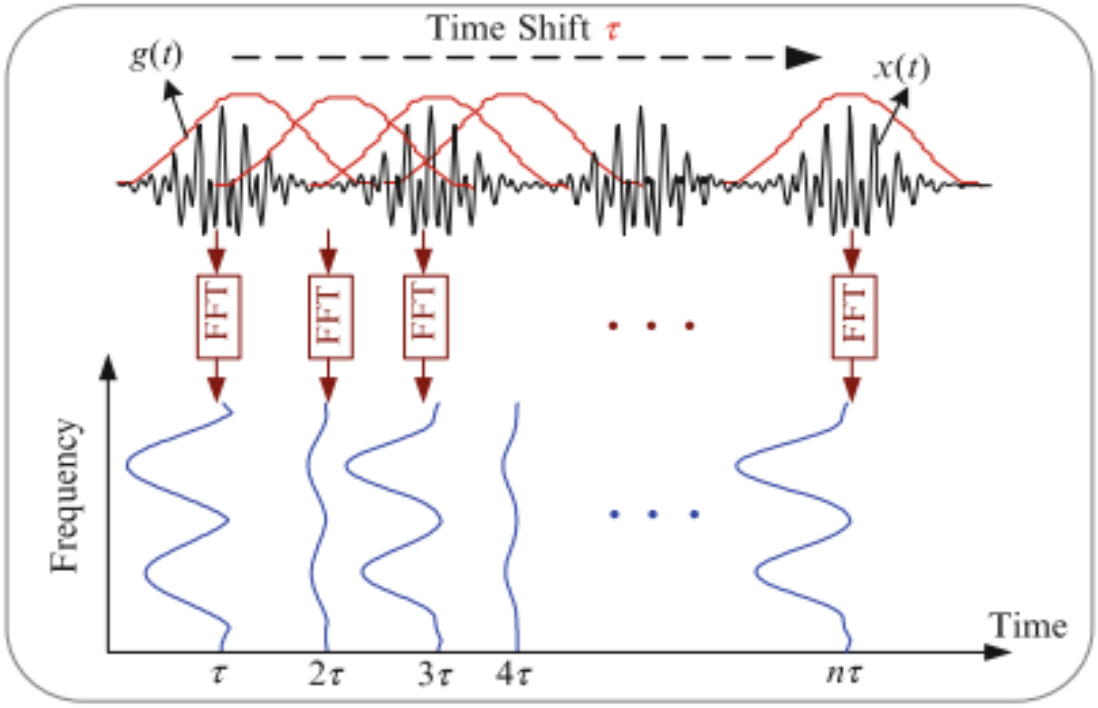

STFT can be expressed as

$$\mathbf{STFT}(\boldsymbol{\tau}, \mathbf{f}) = \langle \mathbf{x}, \mathbf{g_{t,f}} \rangle = \int \mathbf{x(t)} \mathbf{g_{t,f}}^{*}\mathbf{(t)dt} = \int \mathbf{x(t)g(t-\tau)}\, \mathbf{e^{-i2\pi ft}dt}$$

According to the uncertainty principle, the time and frequency resolutions of the STFT technique cannot be chosen arbitrarily at the same time.

$$\boldsymbol{\Delta\tau \cdot \Delta f \geq \frac{1}{4\pi}}$$

$$\boldsymbol{\Delta\tau^2 = \frac{\int \tau^2 |g(\tau)|^2 d\tau}{\int |g(\tau)|^2 d\tau}} \qquad \boldsymbol{\Delta f^2 = \frac{\int f^2 |G(f)|^2 df}{\int |G(f)|^2 df}}$$

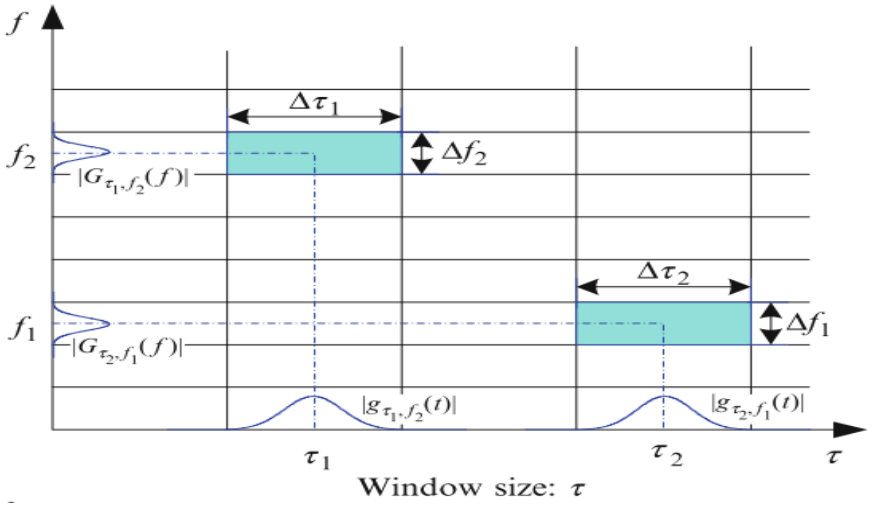

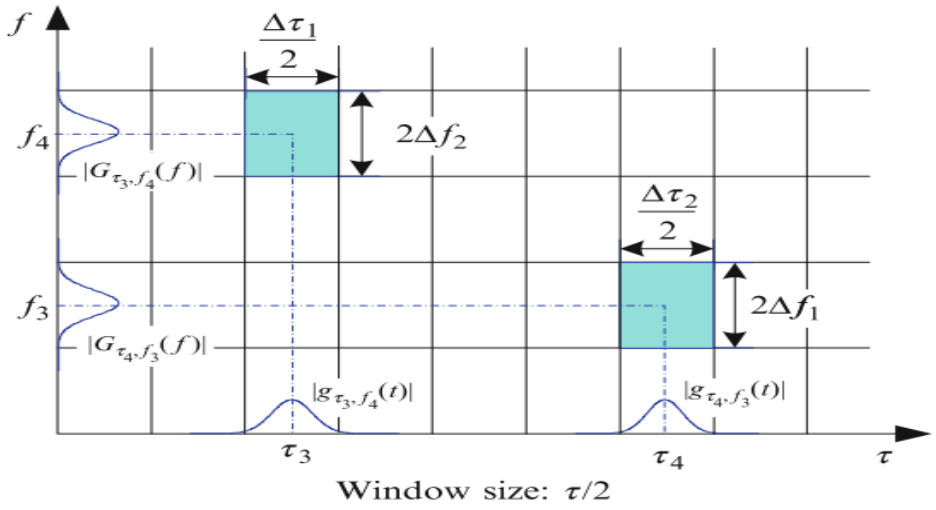

4.5 Wavelet Transform

Wavelet transform is a tool that converts a signal into a different form. This conversion reveals the characteristics hidden in the original signal. The wavelet is a small wave that has an oscillating wavelike characteristic and has its energy concentrated in time.

The first reference to the wavelet goes back to the early twentieth century. Harr's research on orthogonal systems of functions led to the development of a set of rectangular basis functions. The Haar wavelet was named on the basis of this set of functions, and it is also the simplest wavelet family developed till this date.

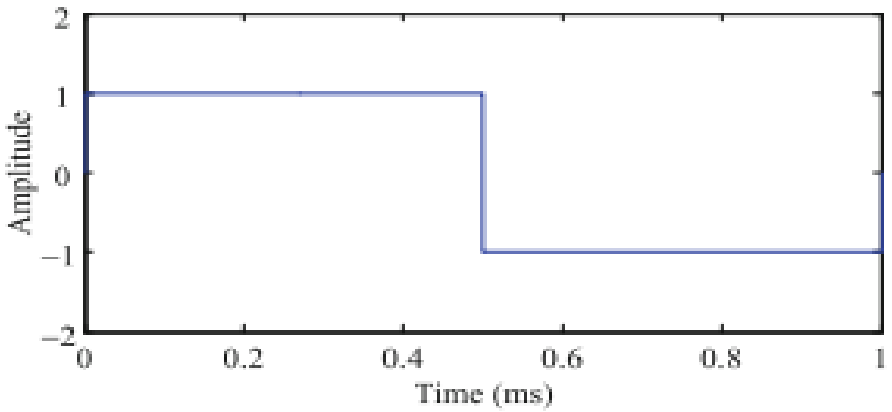

In contrast to STFT, the wavelet transform enables variable window sizes in analyzing different frequency components within a signal. By comparing the signal with a set of functions obtained from the scaling and shift of a base wavelet, it is realized as shown in below Figure

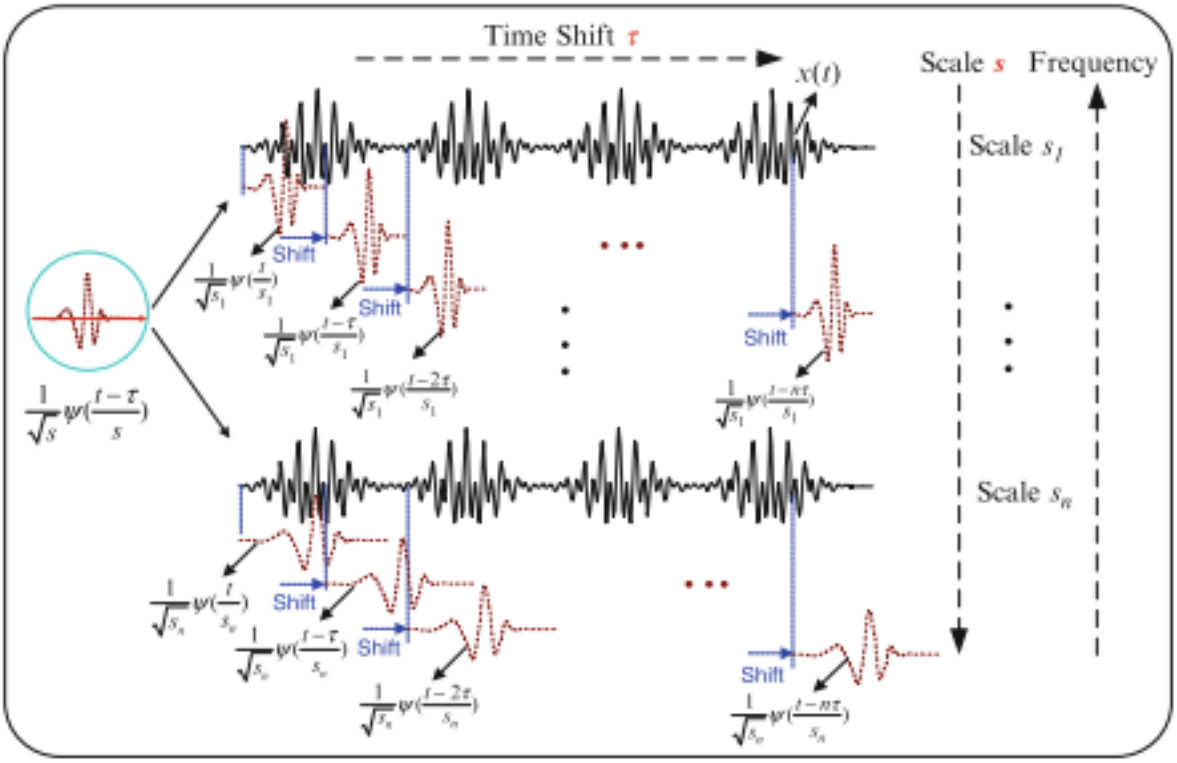

Wavelet transform can be expressed as

$$\mathbf{wt(s.\tau) = \langle x, \Psi_{s,\tau} \rangle = \frac{1}{\sqrt{s}} \int_{-\infty}^{\infty} x(t) \Psi^* \left(\frac{t-\tau}{s} \right) dt}$$

As in below Figure , variations of the time and frequency resolutions of the Morlet wavelet at two locations on the time–frequency plane.

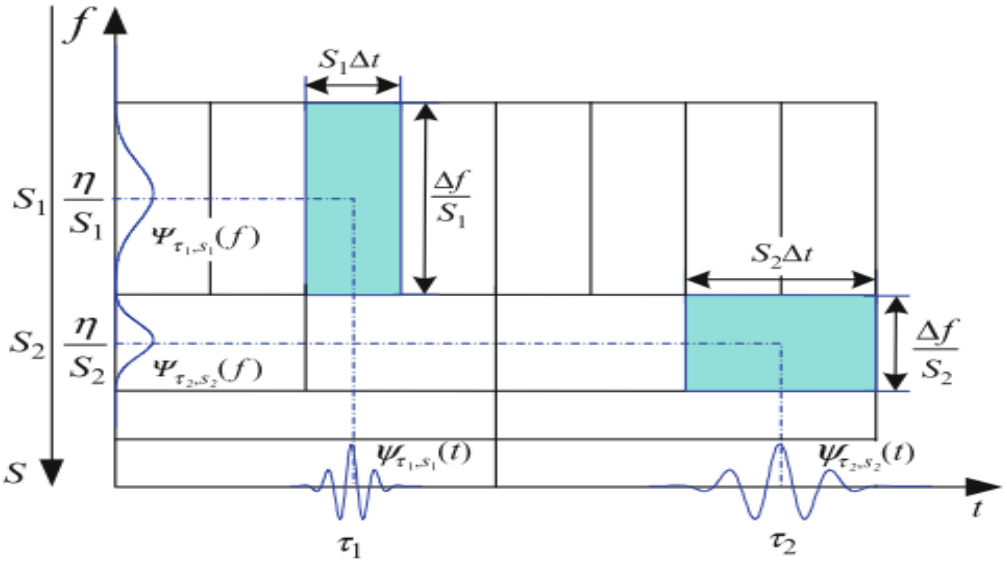

Through variations of the scale and time shifts of the base wavelet function, the wavelet transform can extract the components within over its entire spectrum, by using small scales for decomposing high frequency parts and large scales for low frequency components analysis.

Continuous Wavelet Transform

Properties

The definition of continuous wavelet transform

$$\mathbf{X(a,b) = \frac{1}{\sqrt{b}} \int_{-\infty}^{\infty} x(t) \Psi \left(\frac{t-a}{b} \right) dt}$$

where a shifts time, b modulates the width (not frequency), and□□(t) is mother wavelt.

It has superposition property.

If the continuous wavelet transform of x(t) is X (s, **Ψ**) and of y(t) is Y(s, **Ψ**), then the continuous wavelet transform of z(t) = k1x(t) + k2y(t) can be expressed as

$$\mathbf{Z(s,\tau) = k_1 X(s,\tau) + k_2 Y(s,\tau)}$$

Moreover, it is covariant under translation and dilation.

Suppose that the continuous wavelet transform of x(t) is X (s, $\boldsymbol{\Psi}$), then the transform of x(t-t_0) is

$$\mathbf{X}(\mathbf{s}, \boldsymbol{\tau} - \mathbf{t_0})$$

This means that the wavelet coefficients of x(t-t_0) can be obtained by translating the wavelet coefficients of x(t) along the time with t_0.

On the other hand, suppose that the continuous wavelet transform of x(t) is X (s,□), then the continuous wavelet transform of x(t/a) can be expressed as

$$\sqrt{\mathbf{a}}\mathbf{X}\left(\frac{\mathbf{s}}{\mathbf{a}}, \frac{\boldsymbol{\tau}}{\mathbf{a}}\right)$$

This indicates that, when a signal is dilated by a, its corresponding wavelet coefficients are also dilated by a along the scale and time axes.

1.1.1 Representative Signals

There are several commonly used wavelets for performing the CWT.

One is Maxican hat, which is a normalized second derivative of a Gaussian function, and frequently employed to model seismic data

$$\boldsymbol{\Psi}(\mathbf{t}) = \frac{\mathbf{1}}{\sqrt{\mathbf{2\pi}\boldsymbol{\sigma}^{\mathbf{3}}}}\left(\mathbf{1} - \frac{\boldsymbol{\sigma}^{\mathbf{2}}}{\mathbf{t}^{\mathbf{2}}}\right)\mathbf{e}^{-\frac{\mathbf{t}^{\mathbf{2}}}{\mathbf{2}\boldsymbol{\sigma}^{\mathbf{2}}}}$$

Another is Morlet, which has been used to identify transient components embedded in a signal, bearing defect-induced vibration.

$$\boldsymbol{\Psi}(\mathbf{t}) = \frac{\mathbf{1}}{\sqrt{\boldsymbol{\pi}\mathbf{f_b}}}\mathbf{e}^{\mathbf{i2\pi f_c t}}\mathbf{e}^{-\frac{\mathbf{t}^{\mathbf{2}}}{\mathbf{f_b}}}$$

Another is Frequency B-Spline Wavelet, which has been seen in biomedical signal analysis.

$$\boldsymbol{\Psi}(\mathbf{t}) = \sqrt{\mathbf{f_b}}[\mathbf{sin\ c}\left(\frac{\mathbf{f_b t}}{\mathbf{p}}\right)]^{\mathbf{p}}\ \mathbf{e}^{\mathbf{i2\pi f_c t}}$$

where f_b is the bandwidth parameter, f_c is the wavelet center frequency, and p is an integer parameter.

There are also many other mother wavelets such as Shannon Wavelet (a special case of frequency b-spline wavelet), Gaussian Wavelet, Harmonic wavelet, etc.

Discrete Wavelet Transform

Properties

It can be implemented if it is 1D as shown in below Figure, and 2D case is shown in next Figure. Similarly, it can be fitted into higher dimensionality.

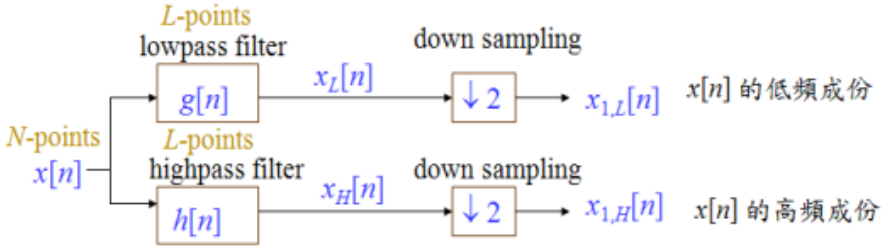

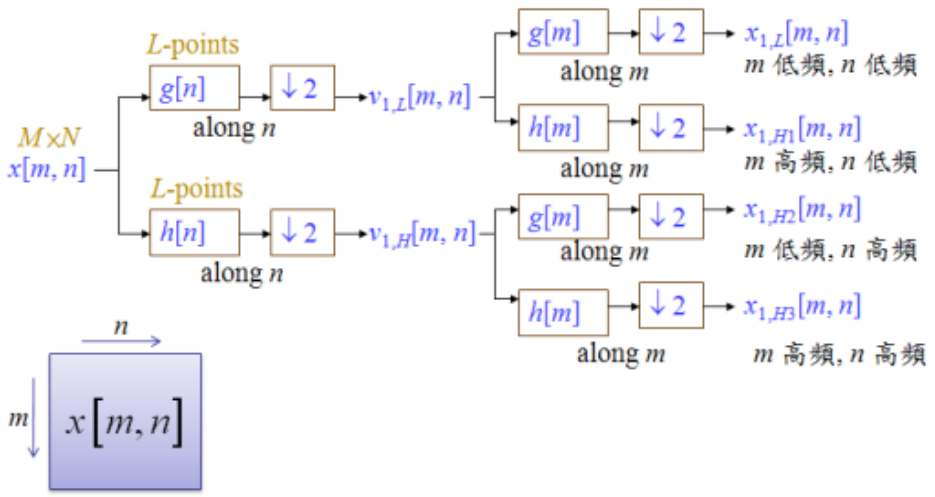

Simply and clearly, we can tell from the implmentation structures that it has higher computational speed than CWT, and the signals would be continuously seperated into low frequencies and high frequencies as shown in below Figure

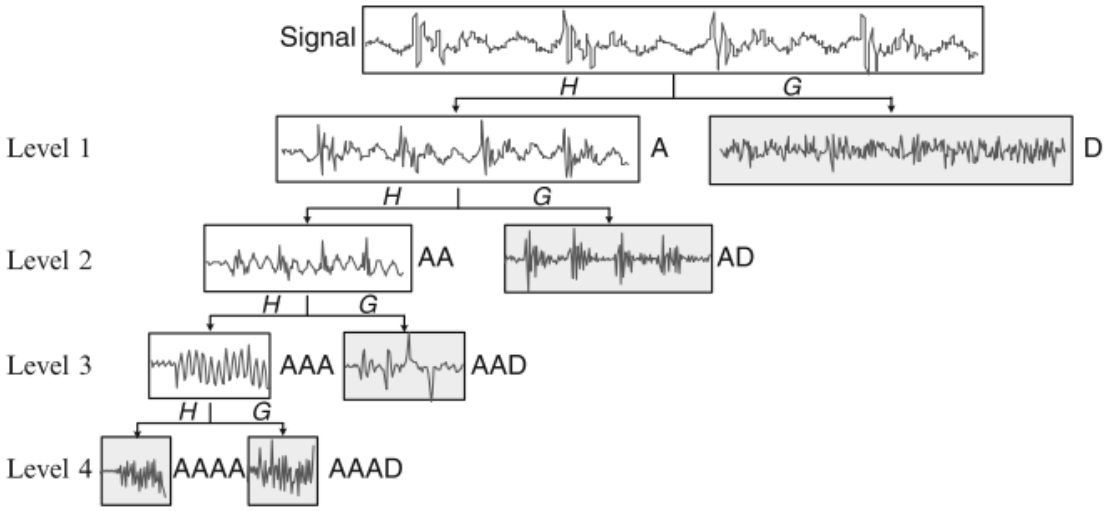

Note: H - Low pass filter; G - High pass filter; A - Approximate information; D - Detailed information

Representative Signals

There are several commonly used wavelets for performing the DWT.
One is Haar, which is orthogonal and symmetric. The property of symmetry ensures that the Haar wavelet has linear phase characteristics, meaning that when a wavelet filtering is performed on a signal with this base wavelet, there will be no phase distortion in the filtered signal. Furthermore, it is the simplest base wavelet with the highest time resolution.

$$\Psi(\mathbf{t}) = \begin{cases} \mathbf{1} & \mathbf{0} \le \mathbf{t} < 0.5 \\ \mathbf{-1} & \mathbf{0.5} \le \mathbf{t} < 1 \\ \mathbf{0} & \mathbf{otherwise} \end{cases}$$

However, the rectangular shape of the Haar wavelet makes its corresponding spectrum with slow decay, leading to a low frequency resolution.
Another is Daubechies, is orthogonal and asymmetric, which introduces a large phase distortion. This means that it cannot be used in applications where a phase information needs to be kept. It is also a compact support base wavelet with a given support width of 2N - 1, in which N is the order of the base wavelet. 2 base and 4 base Daubechies transforms are illustrated in following Figure.

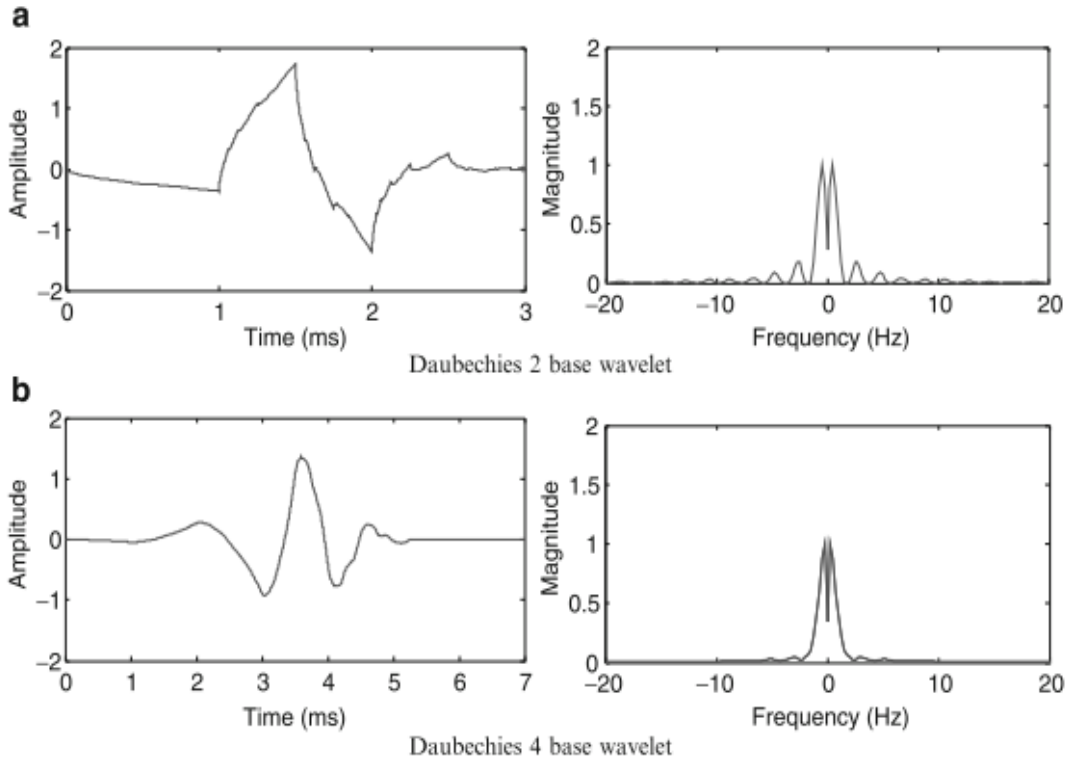

The Daubechies wavelets have been widely investigated for fault diagnosis of bearings and automatic gears.
There are also Coiflet and Symlet, extended from Dauchechies families, but are more symmetric and have vanishing moments in scaling functions.

Selection of Base Wavelet for Biomedical Signals

Overview

One of the advantages of wavelet transform for signal analysis is the abundance of the base wavelets. From such abundance arises a natural question of how to choose a base wavelet that is best suited for analyzing a specific signal. Since the choice in the first place may affect the result of wavelet transform at the end, the question is valid. For example, as shown in above Figure
Therefore, in the following section, we first present a general strategy for base wavelet selection. Then, we introduce several quantitative measures that can be used as guidelines for wavelet selection. While Morlet wavelet is effective in extracting the

impulsive component, the Daubechies and Mexican hat wavelets did not fully reveal the characteristics of impulsive component.

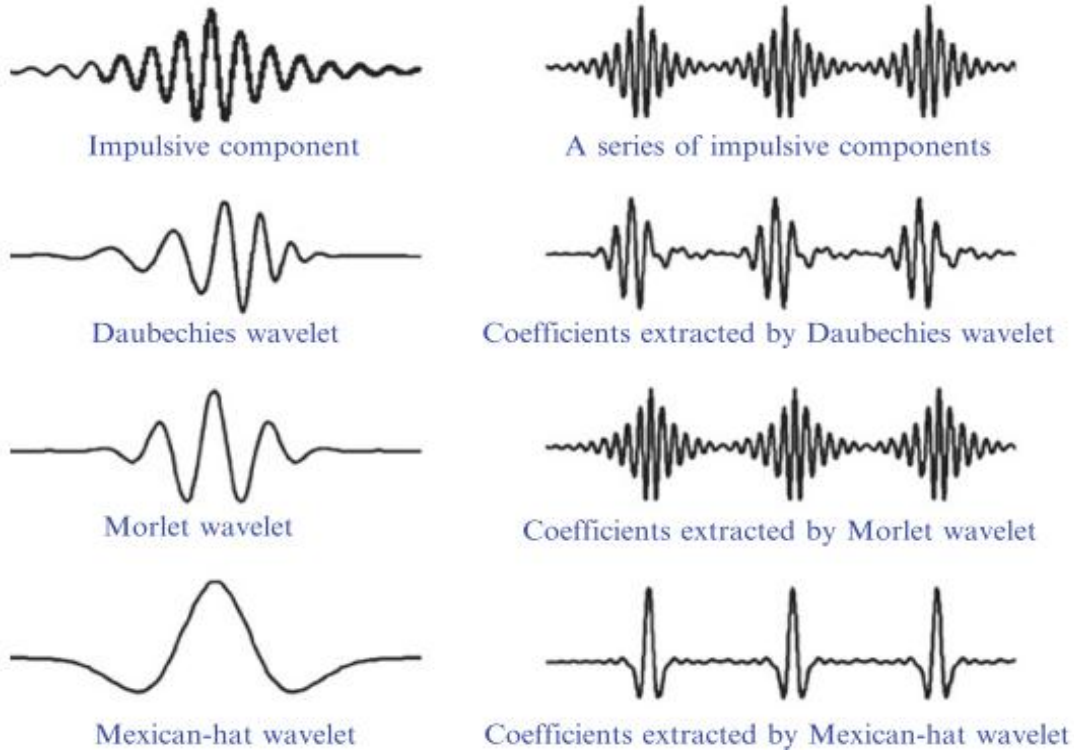

Selection Criteria

There are two ways to measure wavelet performance, one is qualitative and the other is quantitative.

Base wavelets are characterized by orthogonality, symmetry, and compact support. Understanding these properties will help choose a candidate base wavelet from the wavelet families for analyzing a specific signal. For example, the orthogonality property indicates that the inner product of the base wavelet is unity with itself, and zero with other scaled and shifted wavelets. As a result, an orthogonal wavelet is efficient for signal decomposition into nonoverlapping subfrequency bands. The symmetric property ensures that a base wavelet can serve as a linear phase filter. A compact support wavelet is one whose basis function is nonzero only within a finite interval. This allows the wavelet transform to efficiently represent signals that have localized features.

In the area of biomedical engineering, the regularity and symmetry of base wavelets were considered as essential features for auditory-evoked potentials (AEP) signal analysis. The morphology and latency of peaks were preserved with a symmetric base wavelet. By using the properties of compact support, vanishing moment, and orthogonality, the Coiflet wavelet was selected to separate burst andtonic components in the electromyogram (EMG). In addition to orthogonality, the property of complex

or real basis was used to guide the choice of the basewavelet for electrocardiogram (ECG) signal analysis. The Morlet wavelet, Gaussian wavelet, and quadratic B-Spline wavelet were preselected as the candidates for ECG detection and segmentation.
Besides above properties, shape matching is alternative to wavelet selection. For example, to measure the timing of multiunit bursts in surface EMG from single trials, wavelets of different shapes, such as square, triangular, Gaussian and Mexican Hat, were investigated. The Daubechies wavelet was chosen for its similarity to the shape of motor unit potentials hidden in the EMG signal. Also, base wavelets of different shapes were compared with ECG signals to determine their appropriateness for extracting a reference base from corrupted ECG.
As far as shape matching is concerned, it is generally difficult to accurately match the shape of a signal to that of a base wavelet through a visual comparison. These deficiencies motivate the study of quantitative measures for base wavelet selection.
In the area of biomedical engineering, study on horse gait classification has discussed an uncertainty model for wavelet selection. The model combines the fuzzy uncertainty with the probabilistic uncertainty to provide a better measure for choosing base wavelet to improve correct classification of different horse gait signals.
In study on cardiovascular ailments in patients, experiments have revealed the suitability of the Daubechies wavelet at order 8 for the ECG signal denoising, as it has the maximum cross correlation coefficient between the ECG signal and the chosen base wavelets, (Daubechies, Symlet, and Coiflet wavelets).
From above discussion and references, we know that

- Coiflect 4 effectively separated burst and tonic components for EMG.
- Morlet, Gaussian, Paul 4, and quadratic B-Spline wavelets were selected for ECG detection and segmentation.
- Symlet 7, Coifect 3, Coifect 4, and Coifect 5 wavelets have better detection for ECG.
-

Furthermore, there are two more quantitative creteria to determine optimal wavelet base, which are maximum energy and minnimum Shannon entropy.
The energy content of a signal x(t) can be calculated by

$$\mathbf{E} = \int |\mathbf{x(t)}|^{\mathbf{2}}\mathbf{dt}$$

It can also be calculated from its wavelet coefficients wt(s, $\boldsymbol{\Psi}$)

$$\mathbf{E} = \int\int |\mathbf{wt(s,\tau)}|^{\mathbf{2}}\mathbf{dsd\tau}$$

The above equation can be revised as

$$\mathbf{E(s)} = \int |\mathbf{wt(s,\tau)}|^{\mathbf{2}}\mathbf{d\tau}$$

If a major frequency component corresponding to a specific scaling s exists in the signal, then the wavelet coefficients at that scale will have relatively high magnitudes when this major frequency occurs. Thus, the energy related to that component can be extracted from the signal when applying wavelet transform. Therefore, we want a base wavelet that can extract the largest amount of energy from the signal.
The entropy here refers to the entropy of the wavelet coefficients, instead of the one of the signal itself. The energy distribution of the wavelet coefficients can be described by Shannon entropy.

$$\mathbf{E_{entropy}(s)} = -\sum_{\mathbf{i=1}}^{\mathbf{N}} \mathbf{p_i \cdot \log_2 p_i}$$

where p_i is the energy probability distribution of wavelet coefficients

$$\mathbf{p_i} = \frac{|\mathbf{wt}(\mathbf{s}, \mathbf{i})|^2}{\mathbf{E_{entropy}}(\mathbf{s})}$$

From the probability principle, we find the bound of the entropy of the wavelet coefficients.

$$\mathbf{0} \leq \mathbf{E_{entropy}}(\mathbf{s}) \leq \mathbf{log_2\, N}$$

If all the other wavelet coefficients are equal to zero except for one coefficient, the entropy equals to zero. If the probability distribution is uniform, which means all the wavelet coefficients are the same (i.e. 1/N), the entropy equals to log2N. Therefore, the lower the entropy is, the higher energy concentration is.

5. Results

Different results have been taken from different methods.I have taken synthetic ECG which is inbuilt in Matlab.I have added 50 Hz Noise in the synthetic signal.Figure has been plotted after every step.After applying 50 Hz noise,I applied Discreet wavelet transform ,calculated the wavelet coefficients then applied thresholding techniques. Results are shown for different combinations.

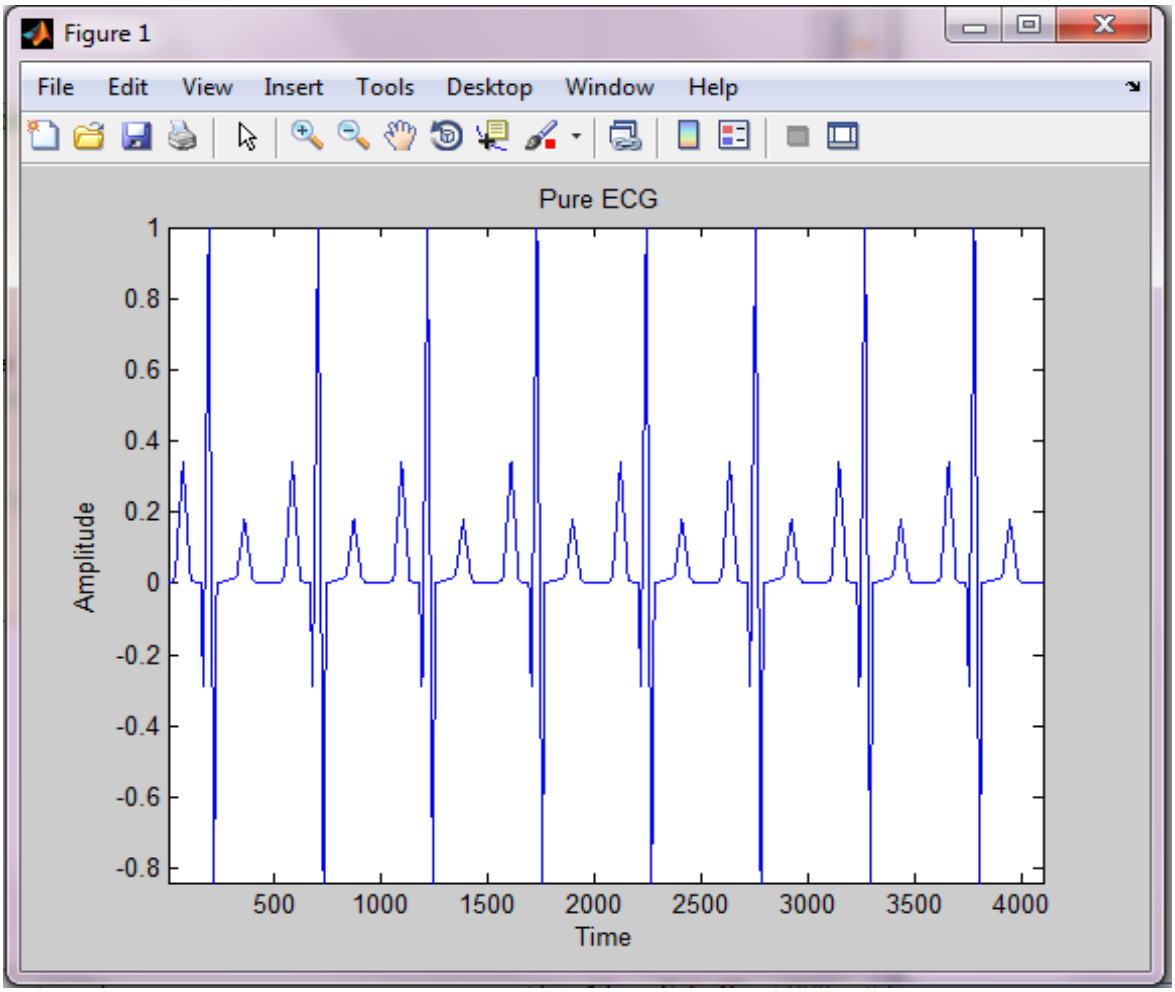

Synthetic ECG waveform

In the above synthetic ECG 50 Hz noise is added in Matlab.Matlab provides toolboxes for various functions and it has special toolbox for wavelet transform.

After going through literature survey various techniques have been used for denoising. 50 Hz noise can not be added with maximum amplitude,so 10% or 20% of the noise can be added.

For adding the dimension of both matrix should be same,otherwise it cannot be added.

Now Noise which are added in ECG has been shown below,

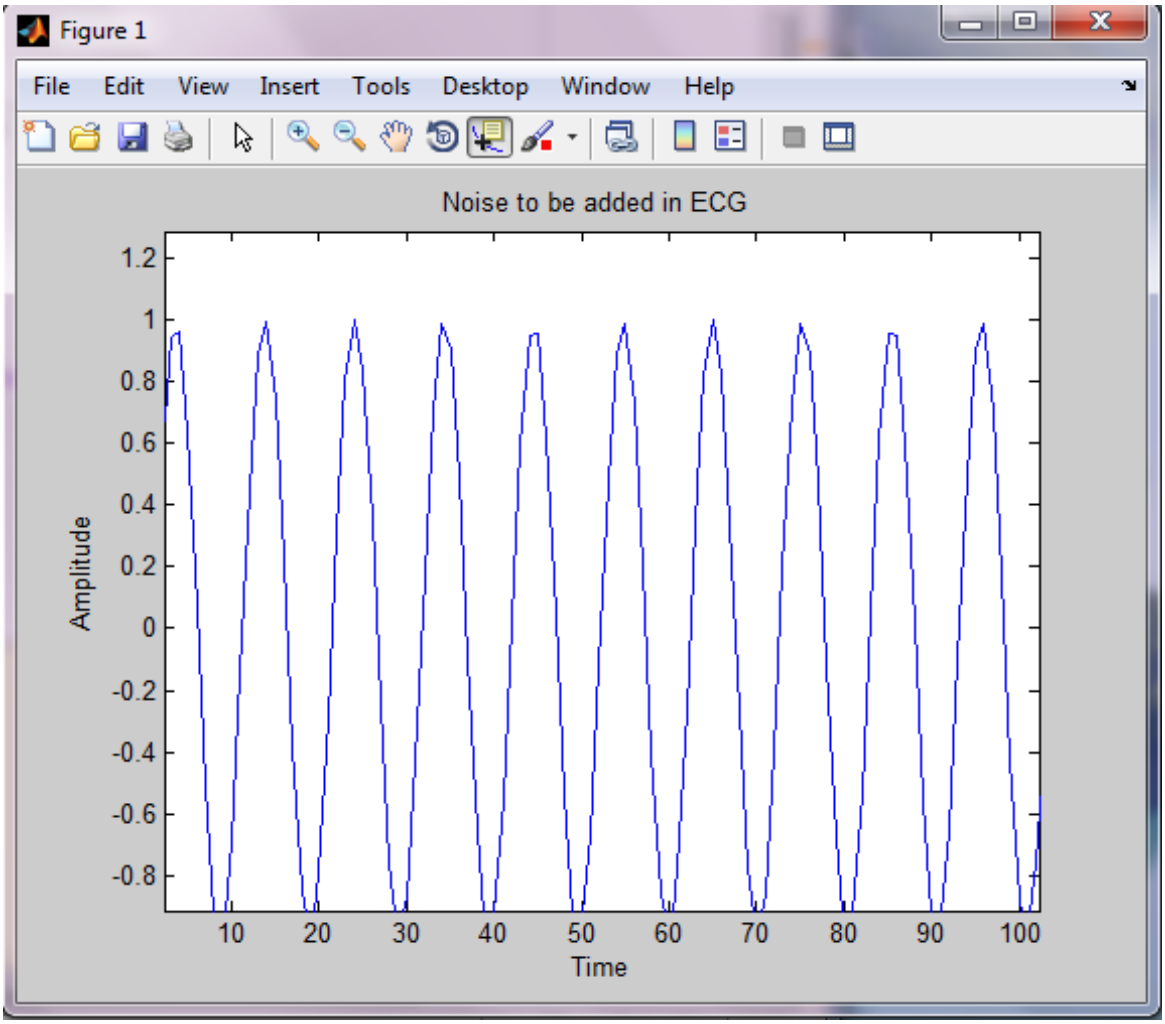

Noise of 50 Hz to be added in Pure ECG

After adding above 50 Hz noise in Pure ECG we can get following ECG waveform.

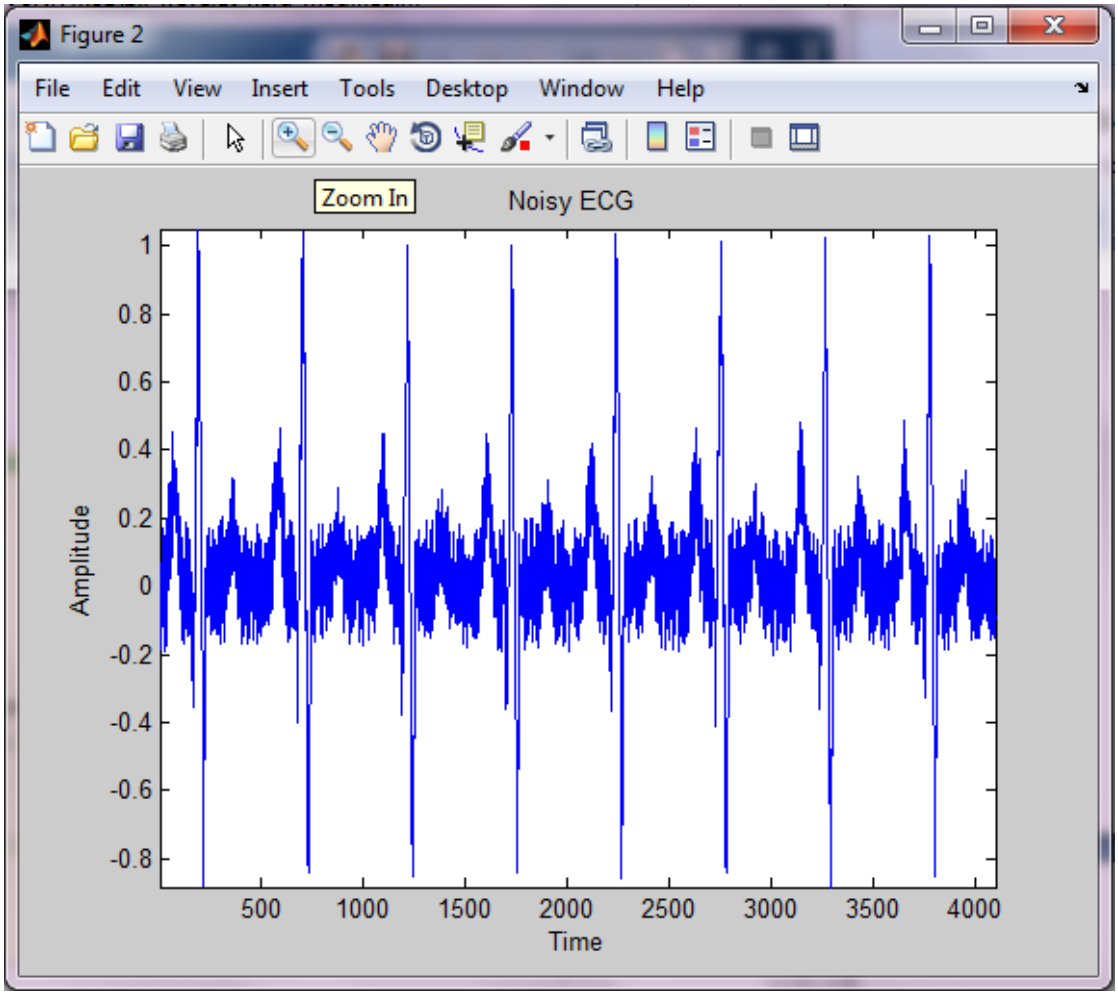

Figure of Noisy ECG

Result for Denoised ECG

After applying Hard Thresholding technique in rbio2.4 wavelet we get the following denoised ECG wave,The SNR,MSE and crosscorrelations of above type of wavelet and thresholding also calculated and shown in the graph.

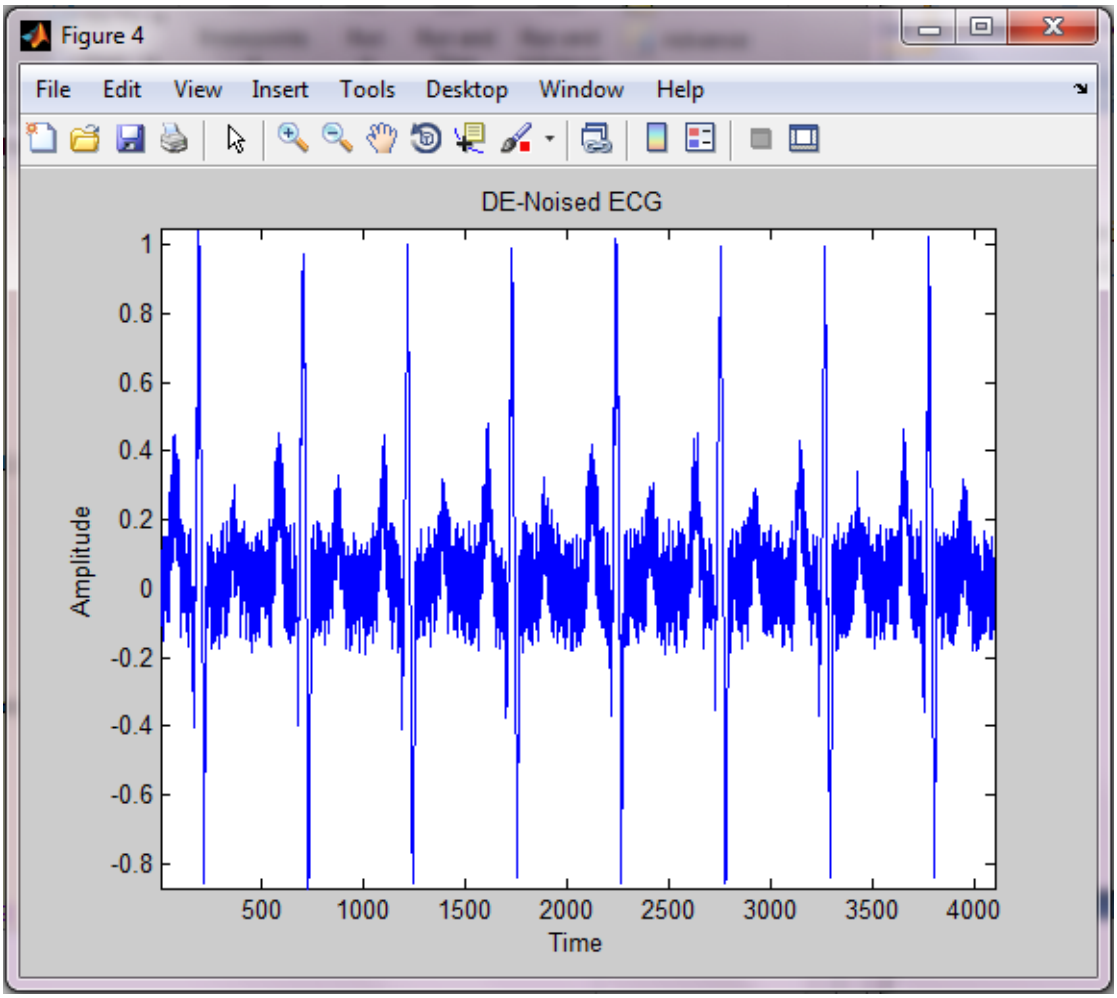

Denoised ECG

The value of SNR,MSE and Cross correlations for rbio2.4 and hard thresholding have been shown in the figure below,

SNR of original signal = 7.9372 dB

MSE of original signal= .0066

SNR of denoised signal = 8.5924 dB

MSE of denoised signal= .0066

Cross correlation of Denoised signal=0.9283

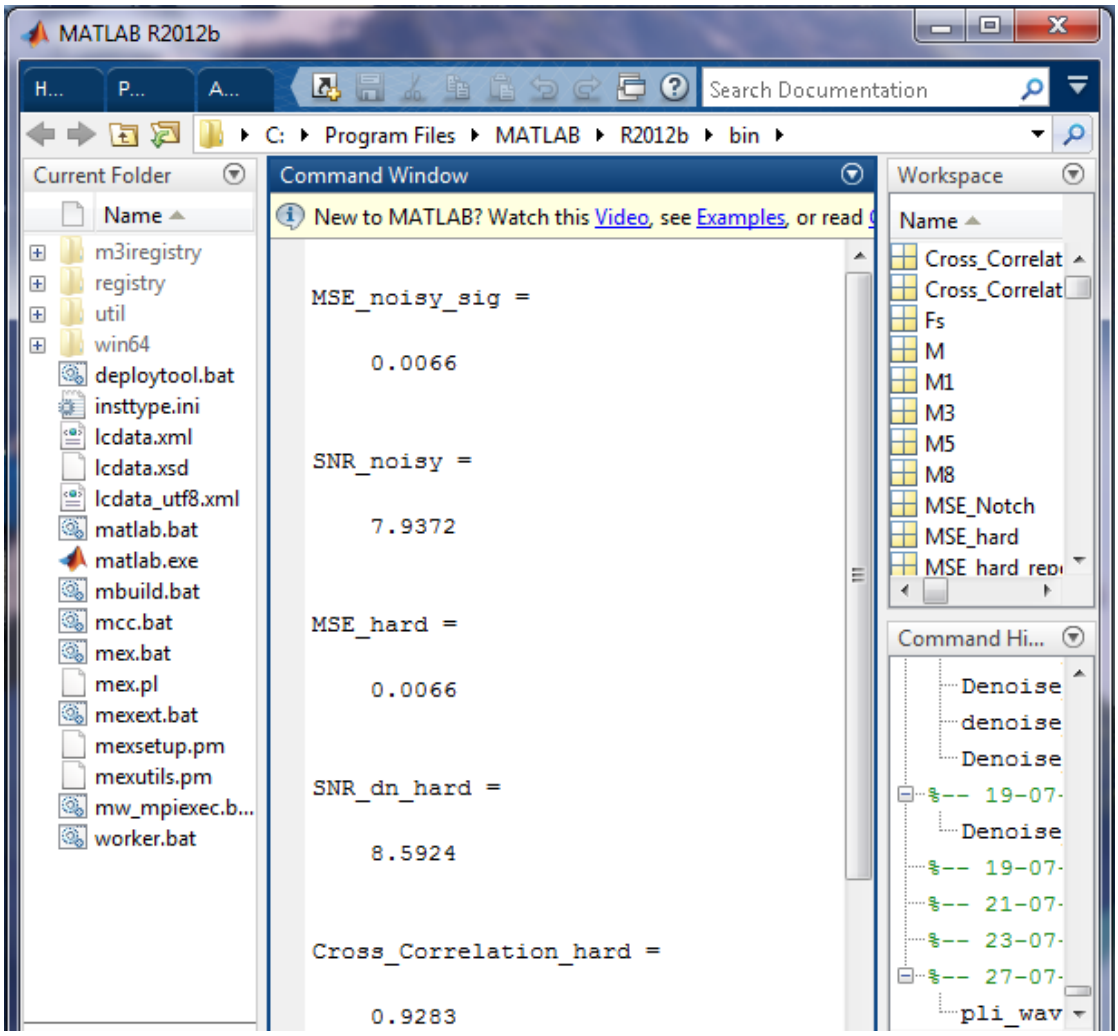

Now we change the thresholding technique,let us choose db9 wavelet and neighborhood thresholding technique, and again we calculate the SNR,MSE and cross correlations value.

Denoised signal using db9 wavelet and neighborhood thresholding;

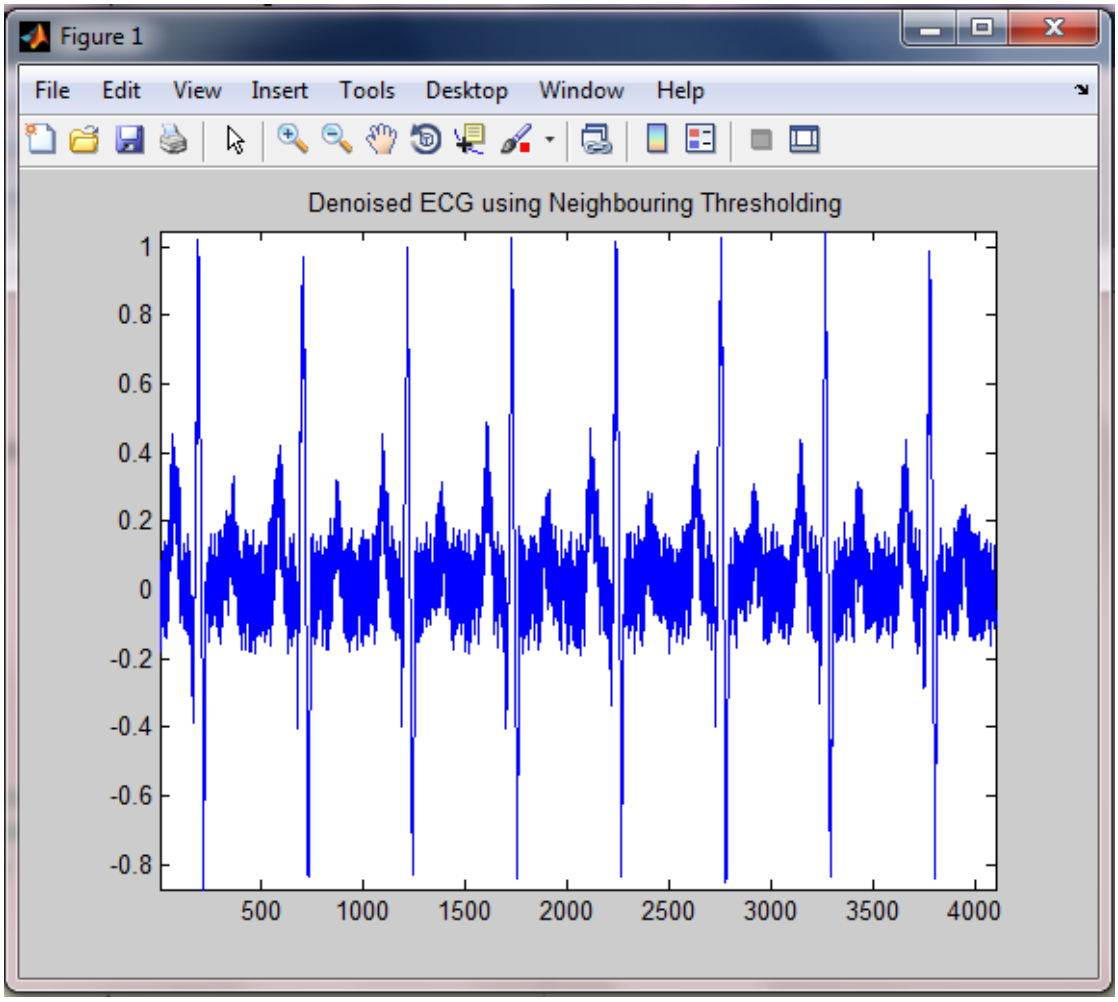

Values for SNR,MSE and Crosscorrelations:

SNR = 8.5663 dB
MSE = .0066
Cross correlation = 0.9278

After going various types of wavelets and thresholding techniques we find out that cross correlation is coming out in order of 0.92 to 0.94 only,now we added Notch filter also and compare the results. Now results are very much improved after applying Notch filter.

Notch Filter

The power line interference (50/60 Hz) is the main source of noise in most of bio-electric signal. We can apply (IIR) notch filter, adaptive notch filtering technique and Discrete Wavelet transform method has been proposed for the removal of power line interference from ECG signal. Different ECG signals from MIT/BIH arrhythmia database are used with added power-line interference noise which is common in ECG signal. The result is analyzed using MATLAB software. Basically two synthesis parameters MSE and SNR have been used. The prime aim of this paper is to adapt the discrete wavelet transform (DWT) to improve the ECG signal quality for better clinical diagnosis.

Methods

The 50Hz power line interference noise is generated & added into the original ECG signal samples taken from the MIT/BIH database. The process of adding noise to original signal is mathematically shown as:

$$F(n) = X(n) + D(n)$$

Where X (n) =Original ECG signal, D (n)=50Hz PLI noise

F (n) =Noisy ECG Signal

IIR Notch Filtering

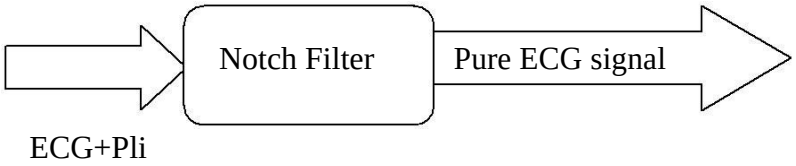

Block diagram of Notch filtering

Fig shows the block diagram of the process of removing power line interference (pli) from the ECG signal. In this diagram it is shown that the corrupted ECG signal which is the mixture of ECG signal & power line interference is passed through a IIR Notch filter. It removes the pli interference & we got the pure ECG signal. In this proposed work instead of FIR Notch filter IIR notch filter is used because the bandwidth of FIR notch filter is wide & it supresses the notch frequency as well as the side frequencies which are unwanted. IIR notch has the sharp notch & it removes only the notch frequency & leave the nearby frequencies (**1**).

Now the following result is with using notch filter which is shown in the diagram, Results are also compared in a chart with and without Notch filter.

De-noising of ECG Signal by Hybrid method of Wavelets and Notch Filter with different thresholding

Table 1: SNR , MSE and Cross correlation values for the de-noising methods using Different wavelets without notch filter

SNR = 7.8717 dB, MSE =0.0067

			Without Notch Filter		
S No.	Wavelet Type	Thresholding	SNR	MSE	Cross Correlation
Symlet Wavelet					
1	Sym1	Hard	8.6265	0.0065	0.9289
2	Sym2	Hard	8.5946	0.0066	0.9283
3	Sym3	hard	8.5165	0.0067	0.9270
4	Sym4	hard	8.5359	0.0067	0.9273
Haar Wavelet					
5	Haar	Hard	8.4855	0.0068	0.9264
Daubechies Wavelet					
6	db1	Hard	8.5156	0.0067	0.9270
7	db2	Hard	8.5011	0.0067	0.9267
8	db4	Hard	8.5866	0.0066	0.9282
			Coiflets Wavelet		
9	Coif1	Hard	8.5282	0.0068	0.9272
10	Coif2	Hard	8.6553	0.0065	0.9294
			BiorSplines wavelet		
11	Bior1.1	Hard	8.4731	0.0068	0.9262
12	Bior2.4	Hard	8.5510	0.0067	0.9276
			Reversebior wavelet		
13	Rbio1.1	Hard	8.6519	0.0066	0.9293
14	Rbio2.4	Hard	8.6900	0.0065	0.9300
			Dmeyer wavelet		
15	dmey	Hard	8.5493	0.0067	0.9275
			Haar Wavelet		
16	Haar	Neighbourhood	13.5667	0.0018	0.9779
			Reversebior wavelet		
	Rbio1.5	Neighbourhood			
17	Rbio1.1	Neighbourhood	13.4876	0.0019	0.9776
18	Rbio1.5	Neighbourhood	13.0528	0.0021	0.9749
19	**Rbio2.4**	**Neighbourhood**	**15.4704**	**0.0012**	**0.9857**
20	**Rbio4.4**	**Neighbourhood**	**12.0177**	**0.0028**	**0.9681**
21	**Rbio2.8**	**Neighbourhood**	**16.3635**	**9.6584e-04**	**0.9884**

22	**Rbio6.8**	**Neighbourhood**		**12.1595**	**0.0026**	**0.9691**
				Daubechies Wavelet		
23	Db1	Neighbourhood		13.5442	0.0018	0.9778
24	Db5	Neighbourhood		12.2713	0.0026	0.9699
25	Db9	Neighbourhood		11.6772	0.0030	0.9654
26	Db13	Neighbourhood		11.8226	0.0029	0.9666
27	Db17	Neighbourhood		11.4028	0.0032	0.9631
				Symlet		
28	Sym1	Neighbourhood		13.6676	0.0018	0.9786
29	**Sym5**	**Neighbourhood**		**11.8001**	**0.0029**	**0.9664**
30	Sym9	Neighbourhood		11.5116	0.0031	0.9641
31	Sym13	Neighbourhood		11.4853	0.0031	0.9638
32	Sym17			11.2624	0.0033	0.9619
	Daubechies Wavelet					
33	Db1	Soft	11.3621	0.0029		0.9645
34	Db5	Soft	14.0623	0.0017		0.9802
35	Db9	Soft	14.4077	0.0016		0.9817
			Symlet Wavelet			
36	Sym5	soft	14.2112	0.0016		0.9809
			Coiflets Wavelet			
37	Coif3	soft	14.2270	0.0016		0.9809
			BiorSplines wavelet			
38	Bior1.1	soft	12.1200	0.0026		0.9690
39	Bior1.5	soft	13.6491	0.0019		0.9782
40	Bior2.4	soft	13.2423	0.0020		0.9760
41	Bior2.8	soft	14.0810	0.0017		0.9803
42	Bior4.4	soft	13.9169	0.0017		0.9795
43	Bior6.8	soft	14.1061	0.0017		0.9804
			Reversebior wavelet			
44	Rbio1.1	soft	12.0410	0.0027		0.9684
45	Rbio1.5	soft	13.8737	0.0017		0.9793
46	Rbio2.4	soft	13.5690	0.0019		0.9778
47	Rbio2.8	soft	14.1384	0.0016		0.9805
48	Rbio4.4	soft	13.8364	0.0018		0.9791
49	Rbio6.8	soft	14.1947	0.0016		0.9808
	Haar wavelet					
50	haar	stein	11.4117	0.0029		0.9644
			Symlet Wavelet			
51	Sym1	stein	11.4098	0.0029		0.9641
52	Sym5	stein	16.6164	8.9791e-04		0.9891
			Coiflets Wavelet			
53	Coif3	stein	17.3955	7.5714e-04		0.9909
			BiorSplines wavelet			
54	Bior1.1	stein	11.4990	0.0029		0.9650
55	Bior1.5	stein	10.6997	0.0038		0.9565

56	Bior2.4	stein	15.7200	0.0011	0.9865
57	Bior2.8	stein	14.3810	0.0015	0.9817
58	Bior4.4	stein	16.5582	9.1391e-04	0.9889
59	Bior6.8	stein	16.7227	8.8070e-04	0.9893
			Reversebior wavelet		
60	Rbio1.1	stein	11.5343	0.0028	0.9653
61	Rbio1.5	stein	15.7717	0.0011	0.9869
62	Rbio2.4	stein	16.7148	8.8772e-04	0.9893
63	Rbio2.8	stein	17.2751	7.7066e-04	0.9906
64	Rbio4.4	stein	16.7933	8.7020e-04	0.9895
65	Rbio6.8	stein	16.8414	8.6199e-04	0.9896

De-noising of ECG Signal by Hybrid method of Wavelets and Notch Filter

Table 1: SNR , MSE and Cross correlation values for the de-noising methods using Different wavelets with notch filter

SNR = 7.9641 dB, MSE =0.0066

			With Notch Filter		
	Wavelet Type	Thresholding	SNR	MSE	Cross Correlation
	Symlet Wavelet				
	Sym1	Hard	11.1919	0.0034	0.9613
	Sym2	Hard	11.3581	0.0033	0.9627
	Sym3	hard	10.0929	0.0044	0.9498
	Sym4	hard	10.3383	0.0042	0.9526
	Haar Wavelet				
	Haar	Hard	11.0658	0.0035	0.9601
			Daubechies Wavelet		
	db1	Hard	11.1478	0.0033	0.9609
	db2	Hard	11.0198	0.0035	0.9597
	db4	Hard	10.1299	0.0044	0.9502
			Coiflets Wavelet		
	Coif1	Hard	10.7256	0.0038	0.9568
	Coif2	Hard	10.1467	0.0044	0.9504
			BiorSplines wavelet		
	Bior1.1	Hard	11.6175	0.0030	0.9650
	Bior2.4	Hard	9.8151	0.0048	0.9464
			Reversebior wavelet		
	Rbio1.1	Soft	10.9449	0.0035	0.9590
	Rbio2.4	Hard	11.3223	0.0033	0.9624
			Dmeyer wavelet		
	dmey	Hard	9.5359	0.0051	0.9427
			Haar Wavelet		
	Haar	Neighbourhood	**13.0001**	**0.0020**	**0.9752**
			Reversebior wavelet		
	Rbio1.1	Neighbourhood	**12.9453**	**0.0021**	**0.9749**
	Rbio1.5	Neighbourhood	**17.2489**	**7.7896e-**	**0.9906**

				04	
	Rbio2.4	**Neighbourhood**	**18.2778**	**6.1091e-04**	**0.9926**
	Rbio4.4	**Neighbourhood**	**17.1580**	**8.0480e-04**	**0.9903**
	Rbio2.8	**Neighbourhood**	**19.5542**	**4.5425e-04**	**0.9945**
	Rbio6.8	**Neighbourhood**	**17.8357**	**6.8356e-04**	**0.9917**
			Daubechies Wavelet		
	Db1	Neighbourhood	13.0661	0.0020	0.9755
	Db5	Neighbourhood	**17.2503**	**7.9234e-04**	**0.9905**
	Db9	Neighbourhood	**16.3399**	**9.7529e-04**	**0.9883**
	Db13	Neighbourhood	**16.9444**	**8.4939e-04**	**0.9898**
	Db17	Neighbourhood	**15.8282**	**0.0011**	**0.9868**
			Symlet		
	Sym1	Neighbourhood	13.1044	0.0020	0.9760
	Sym5	**Neighbourhood**	**16.5138**	**9.2918e-04**	**0.9888**
	Sym9	Neighbourhood	15.9807	0.0011	0.9873
	Sym13	Neighbourhood	16.0727	0.0010	0.9876
			15.3281	0.0012	0.9852
			Daubechies Wavelet/Modified threshold		
	Db1	soft	11.1256	0.0030	0.9627
	Db5	Soft	15.5306	0.0012	0.9859
	Db9	Soft	15.9715	0.0011	0.9873
			Symlet Wavelet		
	Sym5	soft	15.8329	0.0011	0.9869
			Coiflets Wavelet		
	Coif3	soft	15.8372	0.0011	0.9869
			BiorSplines wavelet		
	Bior1.1	soft	12.6199	0.0023	0.9726
	Bior1.5	soft	14.4950	0.0015	0.9821
	Bior2.4	soft	14.6503	0.0014	0.9827
	Bior2.8	soft	15.7409	0.0011	0.9866
	Bior4.4	soft	15.4462	0.0012	0.9856
	Bior6.8	soft	15.7339	0.0011	0.9866
			Reversebior wavelet		
	Rbio1.1	soft	12.5876	0.0023	0.9724
	Rbio1.5	soft	14.9845	0.0013	0.9841
	Rbio2.4	soft	14.9199	0.0014	0.9838

	Rbio2.8	soft	15.7050	0.0011	0.9865
	Rbio4.4	soft	15.2480	0.0013	0.9850
	Rbio6.8	soft	15.9205	0.0011	0.9871
			Haar wavelet		
	haar	soft	11.1731	0.0031	0.9625
			Symlet Wavelet		
	Sym1	stein	11.3572	0.0029	0.9558
	Sym5	stein	19.2723	4.8324e-04	0.9899
			Coiflets Wavelet		
	Coif3	stein	19.1611	5.0000e-04	0.9895
			BiorSplines wavelet		
	Bior1.1	stein	11.4503	0.0029	0.9567
	Bior1.5	stein	12.1304	0.0027	0.9539
	Bior2.4	stein	17.9188	6.7447e-04	0.9863
	Bior2.8	stein	19.2159	4.9185e-04	0.9838
	Bior4.4	stein	18.8947	5.2957e-04	0.9896
			20.1243	3.9896e-04	0.9906
			Reversebior wavelet		
	Rbio1.1	stein	11.4609	0.0028	0.9571
	Rbio1.5	stein	16.6844	8.6475e-04	0.9861
	Rbio2.4	stein	17.5939	7.2068e-04	0.9880
	Rbio2.8	stein	19.6187	4.4652e-04	0.9913
	Rbio4.4	stein	18.2736	6.1468e-04	0.9889
	Rbio6.8	stein	19.9113	4.2151e-04	0.9904

6. Conclusion and Future work

The proposed method can be used for denoising the ECG more accurately as we can see from the above table we can get cross correlation up to 0.99.The ECG signal is properly analysed an errors have been effectively mi nimized.

The baseline and other 50 Hz and their harmonics can be removed by this method.The purpose of this method to get more accurate signal.

Further we can use comb filter to remove the harmonics of 50 hz,but only draw back is that memory space will increase and at the same time processing time also be increased.

I have developed the codes which first generate the synthetic ECG signal in Matlab ,then add the 50 hz noise,then denoise the signal using first discreet wavelet transform then threshold the wavelet coefficient using different combination of wavelets and thresholding,further I have used notch filter to remove the 50 Hz noise.

I have been successful in denoising the ECG as cross correlation comes to 0.99,as shown in the table.

The path breaking research work can be potentially utilized for real time processing and lesser memory occupancy.

7. Bibliography

(1) www.wikipedia.org

(2) The Human Heart retrieved from http://www.venturaes.com

(3) Book "ECG Made easy" by Atul Luthra (Jaypee Pub)

(4) The virtual heart retrieved from http://the virtualheart.org

(5) American heart society retrieved from http://www.americanheart.org

(6) Jennifer Estrada, "Noise Corrupted Signals and Signal Processing using MATLAB".

(7) Ying-Wen Bai, Wen-Yang Chu, Chien-Yu Chen, and Yi-Ting Lee "Adjustable 60Hz Noise Reduction by a Notch Filter for ECG Signals", Instrumentation and Measurement 'Technology Conference Como Italy, IEEE, 18-20 May 2004

(8) James A. Cadzow, "Digital Design Notch Filter Procedure", IEEE Transactions on acoustics, speech, and signal processing, VOL. ASSP-22, NO. 1, FEBRUARY 1974.

(9) Mahesh S. Chavan, R.A. Agarwal, M.D. Uplane, ''Design and implementation of Digital FIR Equi-ripple notch Filter on ECG signal for removal of Power line Interference" WSEAS Transactions on Signal Processing, Volume 4, April 2008, pp: 221-30.

(10) http://www.mathworks.com, "MATLAB MATHWORKS".

(11) http://www.physionet.org/cgi-bin/atm/ATM,"MIT-BIH Arrhythmia Database".

(12) Kotaro Hirano, member, IEEE, Shotard Nishimura, and Sanjit k Mitra, FELLOW, IEEE, "Design of digital notch filter" IEEE Transaction of communication,VOL.COM-22,pp.964_970,No. 7,July 1979

(13) L. Smital Martin, Vıtek, Jirı Kozump and Ivo Provazn, ―Adaptive Wavelet Wiener Filtering of ECG Signals‖, IEEE TRANSACTIONS ON BIOMEDICAL ENGINEERING, VOL. 60, NO. 2, FEBRUARY 2013

(14) S. Poornachandra, ―Wavelet-based denoising using subband dependent threshold for ECG signals,‖ *Digital Signal Process.*, vol. 18, no. 1, pp. 49–55, Jan. 2008

(15) M. Jansen, *Noise Reduction by Wavelet Thresholding*. New York: Springer-Verlag, 2001..